

Triamidostannates(II) as Sterically Demanding Ligands for Rhodium and Iridium

Michaela Kilian, Hubert Wadeppohl, and Lutz H. Gade*

Anorganisch-Chemisches Institut, Universität Heidelberg, Im Neuenheimer Feld 270,
69120 Heidelberg, Germany

Received September 28, 2007

Reaction of the triamidostannates(II) $\text{MeSi}[\text{SiMe}_2\text{N}(3,5\text{-xyl})]_3\text{SnLi}(\text{OEt}_2)$ (**2a**) and $\text{MeSi}[\text{SiMe}_2\text{N}(\text{p-tol})]_3\text{SnLi}(\text{OEt}_2)$ (**2b**) with 0.5 molar equiv of $[\text{RhCl}(\text{COD})]_2$ gave the zwitterionic complexes $[\text{MeSi}[\text{SiMe}_2\text{N}(\text{Aryl})]_2\text{Sn}[\text{SiMe}_2\text{N}(\eta^6\text{-Aryl})\text{Rh}(\text{diolefin})]$ (Aryl = 3,5-xyl: **3a**, p-tol: **3b**). In these one of the aryl groups acts as a η^6 -ligand, thus resulting in the 18-electron rhodium species. Addition of 1 equiv of PPh_3 to a solution of **3a** or **3b** yielded the square-planar complexes $[\text{MeSi}[\text{SiMe}_2\text{N}(\text{Aryl})]_3\text{SnRh}(\text{PPh}_3)(\text{COD})]$ (Aryl = 3,5-xyl: **4a**, p-tol: **4b**), in which the stannates are directly bonded to rhodium through Rh–Sn bonds. Treatment of the complexes **4a,b** and **5a,b** with hydrogen gas in the presence of benzene leads to the hydrogenation of the diolefin and its replacement by benzene as a formal six-electron donor ligand. These 18-electron complexes $[\text{MeSi}[\text{SiMe}_2\text{N}(\text{p-tol})]_3\text{SnRh}(\text{PPh}_3)(\eta^6\text{-arene})]$ **6a,b** and **7a,b** are also accessible by reacting the stannates with 0.5 equiv of $[\text{RhCl}(\text{C}_2\text{H}_4)_2]_2$, PPh_3 , and the appropriate arene. Upon reacting the xylyl stannate **2a** with $[\text{IrCl}(\text{COD})]_2$ and Ph_3P , it was possible to isolate the square-planar Ir complex $[\text{MeSi}[\text{SiMe}_2\text{N}(3,5\text{-xyl})]_3\text{SnIr}(\text{PPh}_3)(\text{COD})]$ (**8a**). In contrast, for the tolyl stannate CH-activation occurred to give the Ir^{III} compound $[\text{MeSi}[\text{SiMe}_2\text{N}(\text{p-tol})]_2[\text{SiMe}_2\text{N}(2\text{-C}_6\text{H}_3\text{-4-CH}_3)]\text{SnIr}(\text{H})(\text{PPh}_3)(\text{COD})]$ (**8b**).

Introduction

Tin(II) halides have found widespread use as cocatalysts in rhodium- and iridium-catalyzed transformations, in particular, hydrogenations and carbonylations.^{1–3} Stannyl fragments may effectively act as SnX_3^- ancillary ligands in $\text{Rh–Sn}^{4–15}$ and

Ir–Sn complexes^{16–24} or may be a photocleavable part of M–Sn catalyst precursors.²⁵ Alternatively, they may temporarily bind to the transition metal during the course of a catalytic cycle in which they act as alkyl or aryl transfer reagents.²⁶

Other than being generated at the transition metal center by insertion of tin(II) reagents into a metal–X bond, such stannyl groups may be used as stable preformed trisubstituted stannates(II), which are then coordinated to the transition metal. This has been the case for the triamidostannates that we developed using tripodal triamido ligands to generate the

* Corresponding author. Fax: (+49) 6221-545609. E-mail: lutz.gade@uni-hd.de.

(1) (a) SnCl_3^- as an ancillary ligand in catalytic reactions. Selected examples: Uson, R.; Oro, L. A.; Fernandez, M. J.; Pinillos, M. T. *Inorg. Chim. Acta* **1980**, *39*, 57. (b) Singer, H.; Umpleby, J. D. *Tetrahedron* **1972**, *28*, 5769. (c) Choudhury, J.; Podder, S.; Roy, S. *J. Am. Chem. Soc.* **2005**, *127*, 6162. (d) Podder, S.; Roy, S. *Tetrahedron* **2007**, *63*, 9146. (e) Uson, R.; Oro, L. A.; Pinillos, M. T.; Arruebo, A.; Ostojica Starzewski, K. A.; Pregosin, P. S. *J. Organomet. Chem.* **1980**, *192*, 227.

(2) Kretschmer, M.; Pregosin, P. S.; Albinati, A.; Togni, A. *J. Organomet. Chem.* **1985**, *281*, 365.

(3) Kaspar, J.; Spogliarich, R.; Graziani, M. *J. Organomet. Chem.* **1982**, *231*, 71.

(4) Werner, H.; Gevert, O.; Haquette, P. *Organometallics* **1997**, *16*, 803.

(5) Veith, M.; Stahl, L.; Huch, V. *Inorg. Chem.* **1989**, *28*, 3278.

(6) Licocchia, S.; Paolesse, R.; Boschi, T.; Bandoli, G.; Dolmella, A. *Acta Crystallogr.* **1995**, *C51*, 833.

(7) Kruber, D.; Merzweiler, K.; Wagner, C.; Weichmann, H. *J. Organomet. Chem.* **1999**, *572*, 117.

(8) Hawkins, S. M.; Hitchcock, P. B.; Lappert, M. F. *J. Chem. Soc., Chem. Commun.* **1985**, 1592.

(9) Garralda, M. A.; Pinilla, E.; Monge, M. A. *J. Organomet. Chem.* **1992**, *427*, 193.

(10) Esteruelas, M. A.; Lahoz, F. J.; Onate, E.; Oro, L. A.; Rodriguez, L. *Organometallics* **1996**, *15*, 3670.

(11) Circu, V.; Fernandes, M. A.; Carlton, L. *Inorg. Chem.* **2002**, *41*, 3859–3865.

(12) Chan, D. M. T.; Marder, T. B. *Angew. Chem.* **1988**, *100*, 436.

(13) Balch, A. L.; Hope, H.; Wood, F. E. *J. Am. Chem. Soc.* **1985**, *107*, 6936.

(14) Carlton, L.; Weber, R.; Levendis, D. C. *Inorg. Chem.* **1998**, *37*, 1264.

(15) Bott, S. G.; Machell, J. C.; Mingos, D. M. P.; Watson, M. J. *J. Chem. Soc., Dalton Trans.* **1991**, 859.

(16) Ruiz, J.; Spencer, C. M.; Mann, B. E.; Taylor, B. F.; Maitlis, P. M. *J. Organomet. Chem.* **1987**, *325*, 253.

(17) Balch, A. L.; Waggoner, K. M.; Olmstead, M. M. *Inorg. Chem.* **1988**, *27*, 4511.

(18) Balch, A. L.; Olmstead, M. M.; Oram, D. E.; Reedy, P. E. Jr.; Reimer, S. H. *J. Am. Chem. Soc.* **1989**, *111*, 4021.

(19) Balch, A. L.; Davis, B. J.; Olmstead, M. M. *Inorg. Chem.* **1990**, *29*, 3066.

(20) Lappert, M. F.; Travers, N. F. *Chem. Commun.* **1968**, 1569.

(21) Uson, R.; Oro, L. A.; Fernandez, M. J.; Pinillos, M. T. *Inorg. Chim. Acta* **1980**, *39*, 57.

(22) (a) Kretschmer, M.; Pregosin, P. S. *Inorg. Chim. Acta* **1982**, *61*, 247. (b) Kretschmer, M.; Pregosin, P. S.; Favre, P.; Schlaepfer, C. W. *J. Organomet. Chem.* **1983**, *253*, 17.

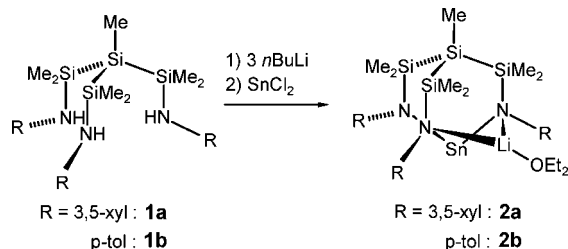
(23) Van der Zeijden, A. A. H.; Van Koten, G.; Wouters, J. M. A.; Wijmuller, W. F. A.; Grove, D. M.; Smeets, W. J. J.; Spek, A. L. *J. Am. Chem. Soc.* **1988**, *110*, 5354.

(24) Moriyama, H. a. P.; Paul, S.; Saito, Y.; Yamakawa; Tetsu. *J. Chem. Soc., Dalton Trans.* **1984**, 2329.

(25) Moriyama, H.; Aoki, S.; Shinoda, S.; Saito, Y. *J. Chem. Soc., Perkin Trans 2* **1982**, 369.

(26) (a) Rh–Sn/Ir–Sn intermediates in catalytic arylations/alkylations: Venkatraman, S.; Li, C.-J. *Tetrahedron Lett.* **2001**, *42*, 4459. (b) Huang, T.; Meng, Y.; Venkatraman, S.; Wang, D.; Li, C.-J. *J. Am. Chem. Soc.* **2001**, *123*, 7451. (c) Oi, S.; Moro, M.; Ito, H.; Honma, Y.; Miyano, S.; Inoue, Y. *Tetrahedron* **2002**, *58*, 91. (d) Masuyama, Y.; Chiyo, T.; Kurusu, Y. *SYNLETT* **2005**, *14*, 2251. (e) Masuyama, Y.; Marukawa, M. *Tetrahedron Lett.* **2007**, *48*, 5963.

Scheme 1



corresponding molecular cages in which the tin donor atom occupies an exposed position.^{27,28}

We have begun to study the triamido stannates as monoanionic equivalents of the ER₃ ligands of the group 15 elements and demonstrated their stability in coordination compounds throughout the d-block.²⁸ Built into the [2,2,2]bicyclooctane cage generated by tripodal amido ligands, these anionic ligands possess large cone angles due to the orientation of the N-substituents. Given the established potential reactivity of their heavier group 9 metal complexes, a systematic study of their coordination chemistry to rhodium and iridium has been carried out.²⁹

As will be demonstrated in this work, N-arylated triamidostannates serve as supporting ligands for different types of rhodium 16e and 18e complexes. Provided that potential cyclometalation of the N-aryl group is suppressed by appropriate substitutions, they are also suitable for the synthesis of Ir^I complexes.

Results and Discussion

Synthesis of the N-Arylated Triamidostannates(II). The triamine precursors of the tripodal triamidostannates(II) were synthesized as reported previously by reaction of MeSi(SiMe₂Cl)₃ with 3 equiv of 3,5-dimethylaniline or *p*-toluidine and an excess of NEt₃ as an auxiliary base to give, respectively, MeSi[SiMe₂NH(3,5-xyyl)]₃ (**1a**) and MeSi[SiMe₂NH(*p*-tol)]₃ (**1b**)³⁰ in good yield. Deprotonation of the amines with *n*-BuLi and treatment with SnCl₂ gave MeSi[SiMe₂N(3,5-xyyl)]₃SnLi(OEt₂) (**2a**) and MeSi[SiMe₂N(*p*-tol)]₃SnLi(OEt₂) (**2b**)^{27c} as described previously for such triamidostannates (Scheme 1).³¹

The ¹H, ¹³C, ²⁹Si, ⁷Li, and ¹¹⁹Sn NMR spectra of **2a** are consistent with an effective 3-fold symmetry caused by the fluxional coordination of the ether-ligated lithium atom in solution. In the solid state this dynamic exchange is frozen, as

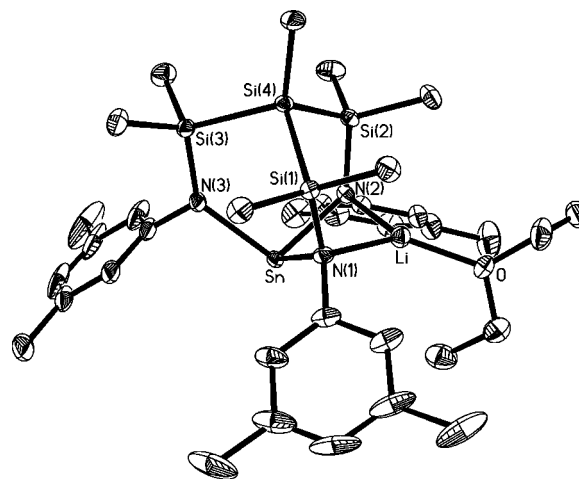


Figure 1. Molecular structure of complex **2a**. Ellipsoids are drawn at the 50% probability level. Principal bond lengths (Å) and angles (deg): N(1)–Li = 2.052(4), N(2)–Li = 2.080(4), Sn–N(1) = 2.2296(17), Sn–N(2) = 2.2204(16), Sn–N(3) = 2.1292(17); N(3)–Sn–N(2) = 102.47(6), N(3)–Sn–N(1) = 103.28(6), N(2)–Sn–N(1) = 82.67(6), Li–N(2)–Sn = 84.55(11), Li–N(1)–Sn = 84.97(12).

is apparent in the molecular structure of **2a**, determined by X-ray diffraction, which is displayed in Figure 1.

The way the lithium ion coordinates to the triamidostannate cage in the structure of **2a** is similar to that previously established for the C₃ chiral trisilylmethane derivative HC[SiMe₂N{(S)-CH(Me)Ph}]₃SnLi(THF).³² The ether-ligated lithium atom bridges two amido N atoms, N(1) and N(2), effectively pulling them together [N(1)–Sn–N(2) 82.67(6)°] and thus widening the angles N(1)–Sn–N(3) (103.28(6)°) and N(2)–Sn–N(3) (102.47(6)°). The tin atom is partially shielded by the xylyl substituents in a characteristic “lamp shade” arrangement.

Synthesis and Structural Characterization of [MeSi[SiMe₂N(Aryl)]₂Sn[SiMe₂N(η⁶-Aryl)]Rh(diolefin) and their Conversion to [MeSi[SiMe₂N(Aryl)]₃SnRh(PPh₃)(diolefin)]. Upon reacting MeSi[SiMe₂N(3,5-xyyl)]₃SnLi(OEt₂) (**2a**) and MeSi[SiMe₂N(*p*-tol)]₃SnLi(OEt₂) (**2b**)^{27c} with 0.5 molar equiv of [RhCl(COD)]₂ at –78 °C, the zwitterionic complexes [MeSi[SiMe₂N(Aryl)]₂Sn[SiMe₂N(η⁶-Aryl)]Rh(diolefin) (Aryl = 3,5-xyyl: **3a**,²⁹ *p*-tol: **3b**) are generated (Scheme 2). Both complexes are thermally unstable but may be isolated by workup at –30 °C. ¹¹⁹Sn NMR spectroscopy gave no evidence for a metal–metal bond between rhodium and tin. For compound **3a** a singlet resonance at –127.8 ppm was detected, the corresponding signal for **3b** being observed at –120.0 ppm. The absence of ¹¹⁹Sn–¹⁰³Rh coupling and the strong shielding of the nuclei indicated the nature of the tin as a stannate(II) and therefore the bonding of the Rh complex fragment to another site of the ligand. In the case at hand, one of the aryl groups acts as a η⁶-ligand, resulting in the 18-electron rhodium species **3a** and **3b**. The tris(arylamido)stannates (**2**) may therefore be seen as adjustable coordinating ligands depending on the electronic properties of the metal.

The η⁶-coordination is indicated by a significant high-field shift for the coordinated aryl proton (**3a**: 5.63 and 4.29 ppm; **3b**: 5.53 and 4.81 ppm) and carbon NMR resonances (**3a**: 151.6, 116.3, 95.4, 92.4 ppm; **3b**: 150.4, 129.4, 103.0, 93.2 ppm).

(27) (a) Examples: Findeis, B.; Gade, L. H.; Scowen, I. J.; McPartlin, M. *Inorg. Chem.* **1997**, *36*, 960. (b) Contel, M.; Hellmann, K. W.; Gade, L. H.; Scowen, I.; McPartlin, M.; Laguna, M. *Inorg. Chem.* **1996**, *35*, 3713. (c) Findeis, B.; Contel, M.; Gade, L. H.; Laguna, M.; Gimeno, M. C.; Scowen, I. J.; McPartlin, M. *Inorg. Chem.* **1997**, *36*, 2386. (d) Lutz, M.; Findeis, B.; Haukka, M.; Pakkanen, T. A.; Gade, L. H. *Organometallics* **2001**, *20*, 2505. (e) Lutz, M.; Galka, C. H.; Haukka, M.; Pakkanen, T. A.; Gade, L. H. *Eur. J. Inorg. Chem.* **2002**, 1968. (f) Lutz, M.; Findeis, B.; Haukka, M.; Graff, R.; Pakkanen, T. A.; Gade, L. H. *Chem.–Eur. J.* **2002**, *8*, 3269. (g) Lutz, M.; Haukka, M.; Pakkanen, T. A.; Gade, L. H. *Organometallics* **2002**, *21*, 3477.

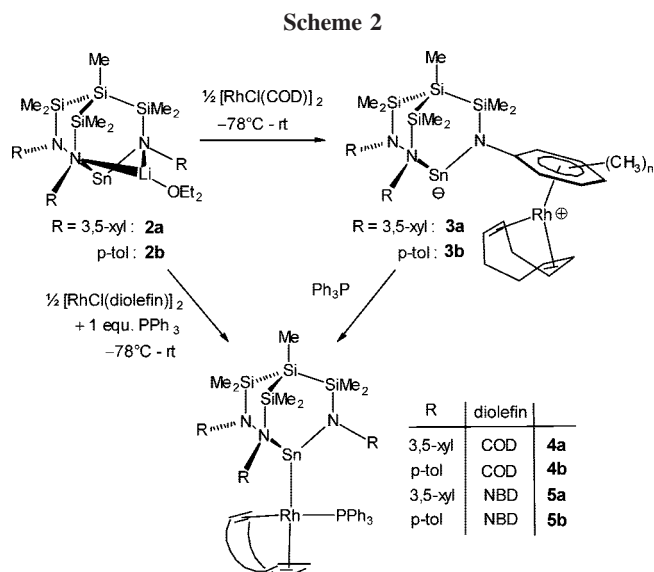
(28) Review on triamidostannates: Gade, L. H. *Eur. J. Inorg. Chem.* **2002**, 1257.

(29) Kilian, M.; Wadepohl, H.; Gade, L. H. *Organometallics* **2007**, *26*, 3076.

(30) Schubart, M.; Findeis, B.; Gade, L. H.; Li, W.-S.; McPartlin, M. *Chem. Ber.* **1995**, *128*, 329.

(31) (a) Hellmann, K. W.; Steinert, P.; Gade, L. H. *Inorg. Chem.* **1994**, *33*, 3859. (b) Hellmann, K. W.; Gade, L. H.; Gevert, O.; Steinert, P.; Lauher, J. W. *Inorg. Chem.* **1995**, *34*, 4069.

(32) Memmler, H.; Kauper, U.; Gade, L. H.; Stalke, D.; Lauher, J. W. *Organometallics* **1996**, *15*, 3637.



Furthermore, the η^6 -arene carbon signals display coupling to rhodium or significant broadening.

An X-ray diffraction analysis of **3a** indicated the assumption of the η^6 -arene coordination in the formally zwitterionic compounds, and its molecular structure is depicted in Figure 2. The arrangement of the xylyl groups with respect to the [2,2,2]bicyclooctane-related stannate cage is quite similar to that of the lithium stannate (**2a**). Moreover, the triamido stannate cage is distorted from an ideal 3-fold symmetry, as is reflected in the N–Sn–N angles [100.11(18)°, 94.61(17)°, and 88.64(17)°], and the aromatic ring of the η^6 -coordinated xylyl group deviates slightly from planarity. Two carbon–rhodium bonds are shorter than the others [C(2)–Rh(1) = 2.208(6) Å, C(5)–Rh(1) = 2.281(6) Å], which is characteristic for the distorted boat configuration of η^6 -coordinated aryls.³³ Whereas there are several reports of η^6 -arene rhodium(I) complexes in the literature,^{8,34–36} the complex [Rh(diphos)(η^6 -PhBPh₃)], prepared by M. Aresta et al.,³⁵ is most closely related. In the latter the cationic rhodium fragment coordinates to an aryl group that is part of the negative ion.

Addition of 1 equiv of PPh₃ to a solution of the zwitterions **3a** and **3b** instantaneously converts them to the square-planar complexes [MeSi[SiMe₂NAr]l₃SnRh(PPh₃)(COD)] (Aryl = 3,5-xylyl: **4a**, p-tol: **4b**), in which the stannate is directly bonded to rhodium through Rh–Sn bonds. This is indicated by the observation of ¹¹⁹Sn–¹⁰³Rh and ¹¹⁹Sn–³¹P coupling in the ¹¹⁹Sn NMR spectra (¹J_{SnRh} = 802 Hz, ²J_{SnP} = 349 Hz for **4a** and ¹J_{SnRh} = 806 Hz, ²J_{SnP} = 311 Hz for **4b**) as well as the coordination shift of the ¹¹⁹Sn NMR resonances to higher field (**4a**: –176.0 ppm, **4b**: –176.5 ppm).

(33) Muetterties, E. L.; Bleeke, J. R.; Wucherer, E. J.; Albright, T. A. *Chem. Rev.* **1982**, *82*, 499.

(34) (a) Uson, R.; Oro, L. A.; Foces-Foces, C.; Cano, F. H.; Vegas, A.; Valderrama, M. J. *Organomet. Chem.* **1981**, *215*, 241. (b) Uson, R.; Oro, L. A.; Foces-Foces, C.; Cano, F. H.; Garcia-Blanco, S.; Valderrama, M. J. *Organomet. Chem.* **1982**, *229*, 293. (c) Singewald, E. T.; Mirkin, C. A.; Levy, A. D.; Stern, C. L. *Angew. Chem.* **1994**, *106*, 2524; *Angew. Chem., Int. Ed.* **1994**, *33*, 2473. (d) Singewald, E. T.; Slone, C. S.; Stern, C. L.; Mirkin, C. A.; Yap, G. P. A.; Liable-Sands, L. M.; Rheingold, A. L. *J. Am. Chem. Soc.* **1997**, *119*, 3048. (e) Werner, H.; Canepa, G.; Ilg, K.; Wolf, J. *Organometallics* **2000**, *19*, 4756. (f) Canepa, G.; Brandt, C. D.; Ilg, K.; Wolf, J.; Werner, H. *Chem.–Eur. J.* **2003**, *9*, 2502.

(35) (a) Albano, P.; Aresta, M.; Manassero, M. *Inorg. Chem.* **1980**, *19*, 1069. (b) Aresta, M.; Quaranta, E.; Albinati, A. *Organometallics* **1993**, *12*, 2032.

(36) Uson, R.; Lahuerta, P.; Reyes, J.; Oro, L. A.; Foces-Foces, C.; Cano, F. H.; Garcia-Blanco, S. *Inorg. Chim. Acta* **1980**, *42*, 75.

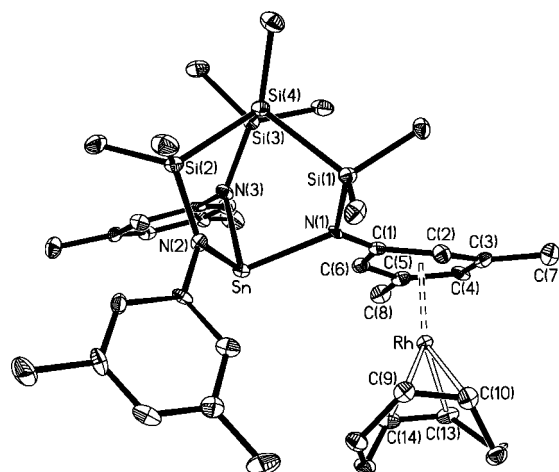


Figure 2. Molecular structure of complex **3a**. Ellipsoids are drawn at the 50% probability level. Principal bond lengths (Å) and angles (deg): N(1)–Sn = 2.263(4), N(2)–Sn = 2.160(4), N(3)–Sn = 2.157(5), C(1)–Rh = 2.458(6), C(2)–Rh = 2.206(6), C(3)–Rh = 2.295(6), C(4)–Rh = 2.300(6), C(5)–Rh = 2.279(6), C(6)–Rh = 2.381(6), C(1)–N(1) = 1.339(7), C(9)–C(10) = 1.402(8), C(13)–C(14) = 1.407(9), C(9)–Rh = 2.115(6), C(10)–Rh = 2.131(6), C(13)–Rh = 2.152(5), C(14)–Rh = 2.169(6); N(1)–Sn–N(2) = 94.64(17), N(1)–Sn–N(3) = 88.66(17), N(2)–Sn–N(3) = 100.13(18).

These 16-electron complexes can also be directly prepared by reacting stannates with 0.5 equiv of the rhodium precursor in the presence of 1 molar equiv of PPh₃ at –78 °C. The NBD derivatives [MeSi[SiMe₂NAr]l₃SnRh(PPh₃)(NBD)] (Aryl = 3,5-xylyl: **5a**, p-tol: **5b**), which tend to be more reactive than their COD analogues, are accessible by this method (Scheme 2). The presence of Sn–Rh bonds is again indicated by coupling of tin with both phosphorus and rhodium (**5a**: ¹J_{SnRh} = 910 Hz, ²J_{SnP} = 349 Hz, **5b**: ¹J_{SnRh} = 910 Hz, ²J_{SnP} = 315 Hz) as well as the low-field shift of the ¹¹⁹Sn NMR signal (**5a**: –146.4 ppm, **5b**: –147.7 ppm).

An X-ray diffraction study of MeSi[SiMe₂N(p-tol)]₃SnRh(PPh₃)(COD) (**4b**) has established the details of its molecular structure, which is displayed in Figure 3. The distance between tin and rhodium is 2.6391(6) Å, which is in the range of previously characterized Sn–Rh bonds.^{4–15} Notable is a slight tilting of the stannate ligand [Si(4)–Sn–Rh = 167.81°] because of steric repulsion of PPh₃ and two tolyl groups. The detailed molecular structures of both **5a** and **5b** have also been established by X-ray diffraction and are shown in Figures 4 and 5.

The structure of **5a** (Figure 4) is very similar to that of **4b** discussed above, the Rh–Sn bond being slightly shorter [2.6242(5) Å] and the angle Si(4)–Sn–Rh is, at 177.27(2)°, closer to the ideal linear arrangement than in the COD derivative. The situation is different in the structure of **5b** depicted in Figure 5. The combination of the sterically less demanding NBD and the *N*-tolyl stannate leads to a reduced interligand repulsion and thus greater flexibility in their arrangement. The result is a more significant tilting of the stannate than in the other derivatives and thus deviation of the Si(4)–Sn–Rh angle [155.67(3)°] from linearity as well as a slightly elongated Rh–Sn bond [2.6522(6) Å].^{4–15}

Synthesis and Structural Characterization of the 18-Electron Complexes [MeSi[SiMe₂N(p-tol)]₃SnRh(PPh₃)(η^6 -arene)]. Treatment of the complexes **4a,b** and **5a,b** with hydrogen gas in the presence of benzene leads to the hydrogenation of the diolefin and its replacement by benzene as a

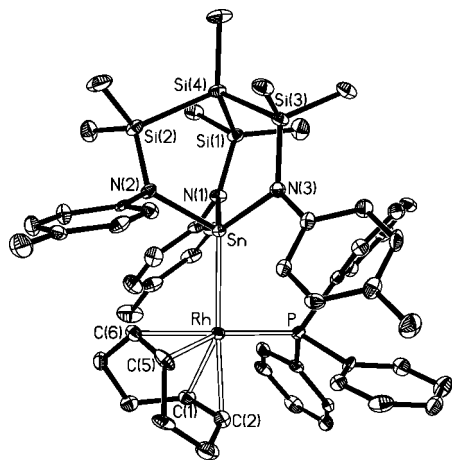


Figure 3. Molecular structure of complex **4b**. Ellipsoids are drawn at the 50% probability level. Principal bond lengths (Å) and angles (deg): Rh–Sn = 2.6391(6), P–Rh = 2.3296(14), N(1)–Sn = 2.129(4), N(2)–Sn = 2.120(4), N(3)–Sn = 2.121(4), C(1)–C(2) = 1.378(8), C(5)–C(6) = 1.367(8), C(1)–Rh = 2.183(5), C(2)–Rh = 2.208(6), C(5)–Rh = 2.208(5), C(6)–Rh = 2.226(5); P–Rh–Sn = 93.89(4), N(1)–Sn–N(2) = 95.78(16), N(1)–Sn–N(3) = 108.25(16), N(2)–Sn–N(3) = 97.85(17), N(1)–Sn–Rh = 108.62(12), N(2)–Sn–Rh = 119.60(12), N(3)–Sn–Rh = 123.07(12), Si(4)–Sn–Rh = 167.81(3).

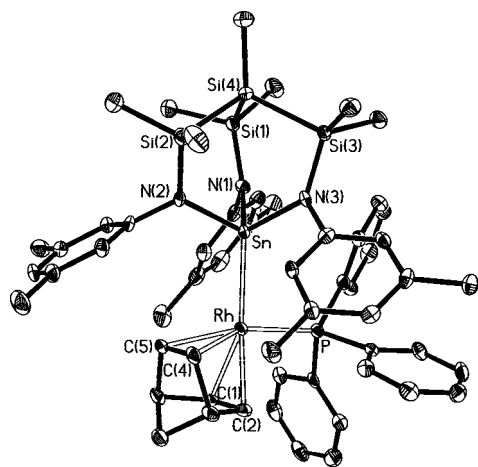


Figure 4. Molecular structure of complex **5a**. Ellipsoids are drawn at the 50% probability level. Principal bond lengths (Å) and angles (deg): Rh–Sn = 2.6242(5), P–Rh = 2.3279(11), N(1)–Sn = 2.113(3), N(2)–Sn = 2.117(3), N(3)–Sn = 2.125(3), C(1)–C(2) = 1.391(7), C(4)–C(5) = 1.365(6), C(1)–Rh = 2.206(4), C(2)–Rh = 2.160(4), C(4)–Rh = 2.186(4), C(5)–Rh = 2.212(4); P–Rh–Sn = 97.43(3), N(1)–Sn–N(2) = 99.25(13), N(1)–Sn–N(3) = 103.73(13), N(2)–Sn–N(3) = 97.08(13), N(1)–Sn–Rh = 113.11(9), N(2)–Sn–Rh = 118.45(10), N(3)–Sn–Rh = 121.72(9), Si(4)–Sn–Rh = 177.27(2).

formal six-electron donor ligand (Scheme 3). Such aryl complexes are also accessible by reacting the stannates **2a** and **2b** with 0.5 equiv of $[\text{RhCl}(\text{C}_2\text{H}_4)_2]$, PPh_3 , and the appropriate arene. It is assumed that the ethylene complexes $[\text{MeSi}[\text{SiMe}_2\text{N}(\text{aryl})]_3\text{SnRh}(\text{PPh}_3)(\text{C}_2\text{H}_4)_2]$ are formed in the first instance; however, they are probably too labile to be isolated or even detected by NMR spectroscopy. In all cases, the 18-electron complexes $[\text{MeSi}[\text{SiMe}_2\text{N}(\text{p-tol})]_3\text{SnRh}(\text{PPh}_3)(\eta^6\text{-arene})]$ **6a,b** and **7a,b** were obtained (Scheme 3). The latter are characterized by large ^{103}Rh – ^{31}P coupling constants (214–215 Hz) compared to those for the square-planar compounds

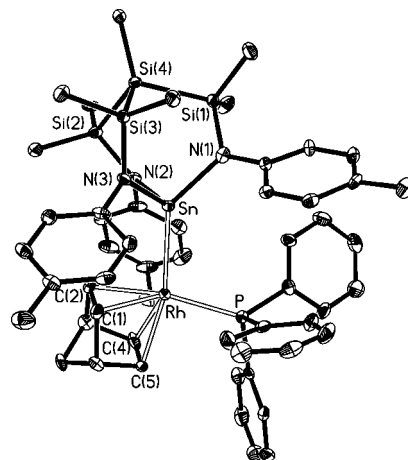
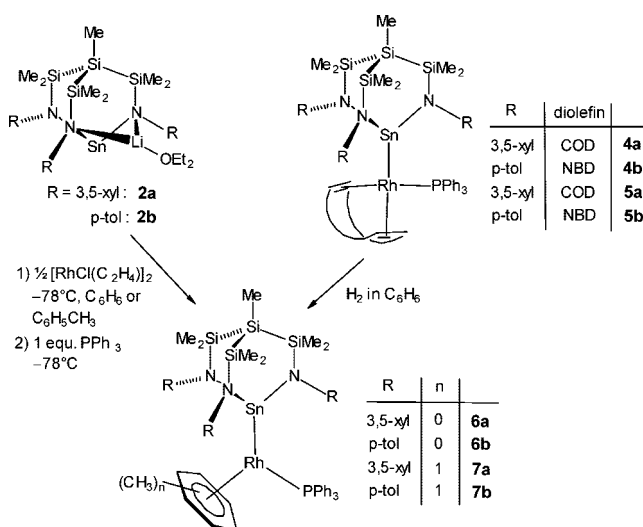


Figure 5. Molecular structure of complex **5b**. Ellipsoids are drawn at the 50% probability level. Principal bond lengths (Å) and angles (deg): Rh–Sn = 2.6522(6), P–Rh = 2.3237(16), N(1)–Sn = 2.117(5), N(2)–Sn = 2.139(5), N(3)–Sn = 2.092(5), C(1)–C(2) = 1.390(9), C(4)–C(5) = 1.377(9), C(1)–Rh = 2.190(6), C(2)–Rh = 2.192(6), C(4)–Rh = 2.177(6), C(5)–Rh = 2.196(6); P–Rh–Sn = 102.67(4), N(1)–Sn–N(2) = 95.83(18), N(3)–Sn–N(1) = 99.74(18), N(3)–Sn–N(2) = 100.03(18), N(1)–Sn–Rh = 133.62(13), N(2)–Sn–Rh = 97.98(13), N(3)–Sn–Rh = 120.84(13), Si(4)–Sn–Rh = 155.67(3).

Scheme 3



(144–159 Hz), a feature that has been previously observed for 18e Rh half-sandwich complexes.^{34–36}

The structural details of the η^6 -benzene derivative **6b** have been established by X-ray diffraction, and its molecular structure is displayed in Figure 6. Similar to other examples previously in the literature,³⁶ the π -coordinated benzene ligand has lost its planarity and adopts a “boat conformation” with two short [C(1)–Rh = 2.266(3), C(4)–Rh = 2.252(3) Å] and four long [C(2)–Rh = 2.312(3), C(3)–Rh = 2.316(3), C(5)–Rh = 2.320(3), C(6)–Rh = 2.333(3) Å] Rh–C distances. The rhodium–tin distance is 2.5833(5) Å and thus shorter than in **4b**, **5a**, and **5b**, while being close to that of the first neutral η^6 -arene-Rh(I)-Sn complex $[\text{Rh}(\eta^6\text{-C}_6\text{H}_5\text{Me})(\text{C}_8\text{H}_{14})\{\text{SnCl}(\text{N}(\text{SiMe}_3)_2)_2\}]$ reported by Lappert et al. [Rh–Sn 2.554(1) Å].⁸

Cyclometalation of the Stannate or Not? Synthesis and Structural Characterization of Ir–Sn Complexes. The synthesis of the iridium analogues of the rhodium diolefin complexes was carried out by a similar procedure by reacting

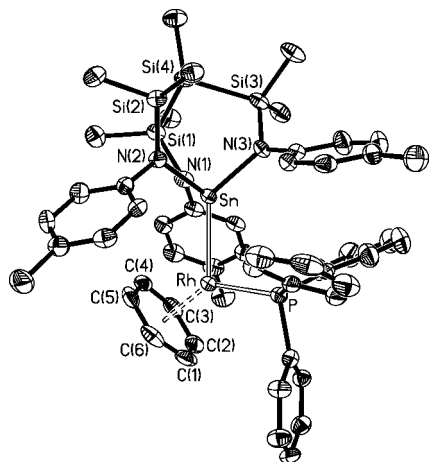


Figure 6. Molecular structure of complex **6b**. Ellipsoids are drawn at the 50% probability level. Principal bond lengths (Å) and angles (deg): Rh–Sn = 2.5833(5), P–Rh = 2.2429(9), N(1)–Sn = 2.139(3), N(2)–Sn = 2.115(2), N(3)–Sn = 2.096(2), C(1)–Rh = 2.266(3), C(2)–Rh = 2.312(3), C(3)–Rh = 2.316(3), C(4)–Rh = 2.252(3), C(5)–Rh = 2.320(3), C(6)–Rh = 2.333(3); P–Rh–Sn = 100.46(3), N(1)–Sn–N(2) = 96.23(10), N(1)–Sn–N(3) = 97.20(10), N(2)–Sn–N(3) = 99.97(10), N(1)–Sn–Rh = 111.37(7), N(2)–Sn–Rh = 115.13(7), N(3)–Sn–Rh = 130.65(7), Si(4)–Sn–Rh = 167.45(2).

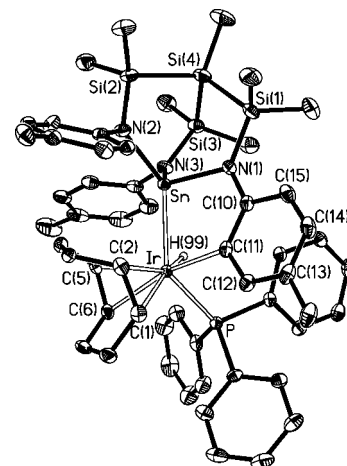
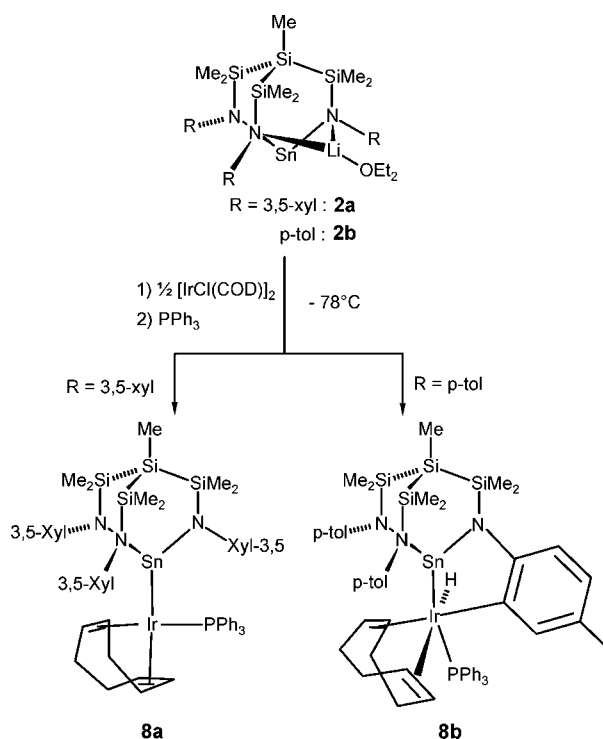


Figure 7. Molecular structure of complex **8b**. Ellipsoids are drawn at the 50% probability level. Principal bond lengths (Å) and angles (deg): Ir–Sn = 2.5798(8), Ir–P = 2.3599(11), Ir–H(99) 1.56(6), N(1)–Sn = 2.074(3), N(2)–Sn = 2.079(3), N(3)–Sn = 2.080(3), C(1)–C(2) = 1.403(5), C(5)–C(6) = 1.385(5), C(1)–Ir = 2.237(3), C(2)–Ir = 2.228(3), C(5)–Ir = 2.271(3), C(6)–Ir = 2.286(3), C(10)–N(1) = 1.423(4), C(11)–Ir = 2.145(3); P–Ir–Sn = 126.87(3), C(11)–Ir–P = 86.26(9), C(11)–Ir–Sn = 79.07(9), N(1)–Sn–N(2) = 103.30(12), N(1)–Sn–N(3) = 105.88(12), N(2)–Sn–N(3) = 98.74(12), N(1)–Sn–Ir = 97.71(8), N(2)–Sn–Ir = 132.82(8), N(3)–Sn–Ir = 115.42(8), Si(4)–Sn–Ir = 159.42(2).

Scheme 4



the stannates with $[\text{IrCl}(\text{COD})]_2$ and Ph_3P . In the case of xylyl stannate **2a** it was possible to isolate the square-planar Ir complex $[\text{MeSi}[\text{SiMe}_2\text{N}(3,5\text{-xyl})]_3\text{SnIr}(\text{PPh}_3)(\text{COD})]$ (**8a**), whereas for the N-tolyl-substituted stannate this product was not formed, but CH-activation occurred to give the Ir^{III} compound $[\text{MeSi}[\text{SiMe}_2\text{N}(\text{p-tol})]_2[\text{SiMe}_2\text{N}(2\text{-C}_6\text{H}_3\text{-4-CH}_3)]\text{SnIr}(\text{H})(\text{PPh}_3)(\text{COD})]$ (**8b**) (Scheme 4).

The resulting hydride in **8b** is detected at -12.23 ppm in the proton NMR spectrum as a doublet ($^2J_{\text{PH}} = 24$ Hz) associated with the tin satellites ($^2J_{\text{SnH}} = 131$ Hz). In the ^{13}C NMR spectrum the signals of the ortho-metallated tolyl substituent are

broad and for the ortho-carbon atom at 130.1 ppm coupling to phosphorus is observed ($^2J_{\text{PC}} = 9.2$ Hz). These spectroscopic features are very similar to those reported for *cis*-(*P,P*)- $[\text{IrH}(\text{PBz}_3)(\text{COD})\{(\text{C}_6\text{H}_4\text{CH}_2)\text{PBz}_2\}]\text{PF}_6$.³⁷ The presence of an iridium–tin bond is confirmed by the ^{119}Sn – ^{31}P coupling ($^2J_{\text{SnP}} = 1713$ Hz), which has been observed in the ^{31}P and ^{119}Sn NMR spectra of compound **8b**.

The coordination geometry at the iridium center of **8b** has been established by X-ray diffraction as (highly) distorted octahedral (Figure 7). The Ir–Sn bond length of 2.5798(8) Å lies in the expected range.^{10–24} The deviation of the rectangular ligand disposition is most pronounced for the Sn–Ir–P angle, which is 126.87(3)°. The iridium atom, the COD, and the hydride as well as C(11) adopt an arrangement that is close to planar. Since the stannate unit is bent toward the cyclometalated part [which is reflected in a Si(4)–Sn–Ir angle of 159.42(2)°], the two remaining tolyl groups point away from the iridium center to make room for COD.

The Ir–H(99) bond length [1.56(6) Å] falls within the range of that in other iridium complexes with terminal hydride ligands [mean 1.573(8) Å of 360 observations currently in the Cambridge Crystallographic Database].

Conclusions

This study has established the use of the tripodal triamido stannates(II) as very bulky ligands for the heavier group 9 metals. While their aryl periphery may act as an initial binding site for rhodium, they remain stable in the subsequent transformations at this metal. Coordination to iridium may occur with concomitant cyclometalation, a reaction that is avoided by introduction of suitably placed substituents in the peripheral aryl groups as in the 3,5-xylyl unit in compound **8a**. To which extent

(37) Landaeta, V. R.; Peruzzini, M.; Herrera, V.; Bianchini, C.; Sanchez-Delgado, R. A.; Goeta, A. E.; Zanobini, F. *J. Organomet. Chem.* **2006**, *691*, 1039.

the triamido stannates(II) tolerate other transformations is currently being studied and will determine their usefulness as ancillary ligands for the late transition metals.

Experimental Section

General Experimental Procedures. All manipulations were performed under an inert gas atmosphere of dried argon (desiccant P₄O₁₀, Granusic, J.T. Baker) in standard (Schlenk) glassware or by working in a glovebox. All reaction flasks were heated prior to use by way of three evacuation-refill cycles. Solvents and solutions were transferred by canula-septa techniques. Solvents were dried according to standard methods, saturated with argon, and stored over potassium mirrors. MeSi(SiMe₂Cl)₃,³⁰ [RhCl(COD)]₂,³⁸ [RhCl(NBD)]₂,³⁹ [RhCl(C₂H₄)₂]₂,⁴⁰ and [IrCl(COD)]₂⁴¹ were synthesized according to literature procedures. The rhodium and iridium precursors were dried over MgSO₄ as solutions in dichloromethane and subsequently precipitated by adding hexane. All other reagents were commercially available and used as received. ¹H, ⁷Li, ¹³C, ²⁹Si, ³¹P, and ¹¹⁹Sn NMR spectra were recorded on a Bruker DRX 200, Avance II 400, or Avance III 600. NMR spectra are quoted in ppm relative to tetramethylsilane (¹H and ¹³C); ⁷Li, ²⁹Si, ³¹P, and ¹¹⁹Sn NMR data are listed in ppm relative to an external standard [⁷Li: LiCl_{aq}, ²⁹Si: Si(CH₃)₄, ³¹P: 85% H₃PO₄, and ¹¹⁹Sn: Sn(CH₃)₄]. ¹H and ¹³C NMR spectra were referenced internally using the residual protonated solvent peak (¹H) or the carbon resonance (¹³C). Infrared spectra were recorded on a Varian 3100 FT-IR spectrometer. Elemental analyses were carried out in the microanalytical laboratory of the chemistry department of Heidelberg.

Preparation of the Compounds. MeSi[SiMe₂NH(3,5-xy)]₃ (1). To a solution of 8.11 mL (64.9 mmol) of 3,5-dimethylaniline and NEt₃ (10.1 mL) in Et₂O (60 mL) was added slowly at 0 °C a solution of 7.01 g (21.6 mmol) of MeSi(SiMe₂Cl)₃ in Et₂O (70 mL). The suspension was warmed to room temperature within 18 h. Then the solvent was removed in vacuo and the residue was suspended in pentane. It was filtered and the solid was washed three times with pentane. The filtrate was concentrated under reduced pressure to about 20 mL and stored at -80 °C. Compound **1** was obtained as an off-white solid (10.97 g, 88%). FT-IR (KBr-disk): 3368 (m, br), 3022 (m), 2952 (s), 2918 (m), 2895 (m), 1597 (s), 1479 (m), 1329 (m), 1250 (s), 1176 (m), 1031 (s, br), 828 (s, br), 770 (s, br), 687 (m), 651 (m) cm⁻¹. ¹H NMR (399.9 MHz, C₆D₆): δ 6.42 (s, 3H, 4-*H*_{xy}), 6.26 (s, 6H, 2,6-*H*_{xy}), 3.32 (s, 3H, *NH*), 2.18 (s, 18H, C₆H₃(C H₃)₂), 0.49 (s, 3H, SiC H₃), 0.42 (s, 18H, Si(CH₃)₂). ¹³C NMR (100.6 MHz, C₆D₆): δ 147.6 (s, 1-*C*_{xy}), 138.8 (s, 3,5-*C*_{xy}), 120.5 (s, 4-*C*_{xy}), 115.1 (s, 2,6-*C*_{xy}), 21.6 (s, C₆H₃(CH₃)₂), 1.7 (s, Si(CH₃)₂), -9.8 (s, SiCH₃). ²⁹Si NMR (79.4 MHz, C₆D₆): δ -2.1 (s, SiMe₂), -88.2 (s, SiMe). Anal. Calcd for C₃₁H₅₁N₃Si₄ (578.1): C, 64.41; H, 8.89; N, 7.27. Found: C, 63.85; H, 8.93; N, 7.41.

MeSi[SiMe₂N(3,5-xy)]₃SnLi(OEt)₂ (2a). A 1.996 g (3.45 mmol) amount of MeSi[SiMe₂NH(3,5-xy)]₃ (**1**) was dissolved in Et₂O and cooled to -78 °C. A 2.5 M solution of *n*-BuLi (4.5 mL, 11.25 mmol) was added. After 2 h at room temperature it was cooled again to -78 °C and the yellow solution was transferred onto 655 mg (3.45 mmol) of solid SnCl₂. The orange suspension was allowed to warm to room temperature and stirred for 18 h. After removal of the solvent in vacuo the red residue was extracted three times with hexane. The combined extracts were concentrated in vacuo to about 10 mL, and storing at -80 °C yielded a pale yellow solid that was washed three times with hexane (1.086 g, 41% yield). FT-IR (KBr-

disk): 3021 (w), 2950 (w), 2917 (w), 1599 (s), 1479 (w, br), 1352 (m), 1246 (m), 1179 (m), 1048 (w), 958 (w), 844 (m), 825 (s), 722 (m), 689 (w), 654 (w) cm⁻¹. ¹H NMR (399.9 MHz, C₆D₆): δ 6.91 (s, 6H, 2,6-*H*_{xy}), 6.60 (s, 3H, 4-*H*_{xy}), 3.03 (q, ³*J*_{HH} = 7.1 Hz, 8H, O(CH₂CH₃)₂), 2.22 (s, 18H, C₆H₃(CH₃)₂), 0.67 (t, ³*J*_{HH} = 7.1 Hz, 12H, O(CH₂CH₃)₂), 0.58 (s, 18H, Si(CH₃)₂), 0.27 (s, 3H, SiCH₃). ⁷Li NMR (155.4 MHz, C₆D₆): δ -1.14 (s). ¹³C NMR (100.6 MHz, C₆D₆): δ = 153.3 (s, 1-*C*_{xy}), 138.2 (s, 3,5-*C*_{xy}), 126.0 (s, 4-*C*_{xy}), 123.4 (s, 2,6-*C*_{xy}), 66.0 (s, O(CH₂CH₃)₂), 21.6 (s, C₆H₃(CH₃)₂), 14.1 (s, O(CH₂CH₃)₂), 4.3 (s, Si(CH₃)₂), -14.5 (s, SiCH₃). ²⁹Si NMR (79.4 MHz, C₆D₆): δ -2.5 (s, SiMe₂), -96.4 (s, SiMe). ¹¹⁹Sn-NMR (149.1 MHz, C₆D₆): δ = -108.7 (s). Anal. Calcd for C₃₅H₅₈LiN₃OSi₄Sn (774.8): C, 54.25; H, 7.54; N, 5.42. Found: C, 54.46; H, 7.84; N, 5.45.

[MeSi[SiMe₂N(3,5-xy)]₃Sn[SiMe₂N(η⁶-3,5-xy)]Rh(COD)] (3a). A 300 mg (0.39 mmol) sample of MeSi[SiMe₂N(3,5-xy)]₃SnLi(OEt)₂ (**2a**) and 95 mg (0.19 mmol) [RhCl(COD)]₂ were suspended in precooled toluene at -78 °C. The orange suspension was stirred for 30 min in the cold before it was warmed to room temperature and centrifuged. Then the centrifugate was concentrated in vacuo and stored at -30 °C to precipitate **3a** as a yellow solid (304 mg, 87%). It was possible to obtain single crystals suitable for X-ray diffraction analysis at -30 °C out of a concentrated solution in toluene. FT-IR (KBr-disk): 3019 (w), 2940 (w), 2884 (w), 1597 (m), 1581 (m), 1532 (w), 1505 (m), 1459 (m), 1345 (s), 1301 (s), 1238 (m), 1195 (w), 1173 (m), 1159 (m), 1037 (w) 961 (w), 874 (m), 852 (m), 827 (m), 775 (m), 703 (w), 640 (m) cm⁻¹. ¹H NMR (399.9 MHz, C₆D₆): δ 7.04 (s, 4H, 2,6-*H*_{xy}), 6.58 (s, 2H, 4-*H*_{xy}), 5.63 (s, 2H, 2,6-*H*_{η⁶-xy}), 4.29 (s, 1H, 4-*H*_{η⁶-xy}), 3.62 (s, br, 4H, CH₂COD), 2.30 (s, 12H, C₆H₃(CH₃)₂), 2.06-1.96 (m, 4H, CH₂ COD), 1.68-1.58 (m, 4H, CH₂ COD), 1.23 (s, 6H, η⁶-C₆H₃(CH₃)₂), 0.85 (s, 6H, Si(CH₃)₂), 0.67 (s, 6H, Si(CH₃)₂), 0.65 (s, 6H, Si(CH₃)₂), 0.37 (s, 3H, SiCH₃). ¹³C NMR (100.6 MHz, C₆D₆): δ 155.4 (s, 1-*C*_{xy}), 151.6 (s, br, 1-*C*_{η⁶-xy}), 137.8 (s, 3,5-*C*_{xy}), 123.6 (s, 2,6-*C*_{xy}), 121.2 (s, 4-*C*_{xy}), 116.3 (d, ¹*J*(¹⁰³Rh-¹³C) = 3.4 Hz, 3,5-*C*_{η⁶-xy}), 95.4 (s, br, 2,6-*C*_{η⁶-xy}), 92.4 (d, ¹*J*(¹⁰³Rh-¹³C) = 3.3 Hz, 4-*C*_{η⁶-xy}), 77.6 (d, ¹*J*(¹⁰³Rh-¹³C) = 13.0 Hz, CH₂COD), 31.8 (s, CH₂ COD), 21.9 (s, C₆H₃(CH₃)₂), 18.7 (s, η⁶-C₆H₃(CH₃)₂), 4.4 (s, Si(CH₃)₂), 4.1 (s, Si(CH₃)₂), 3.3 (s, Si(CH₃)₂), -13.5 (s, SiCH₃). ²⁹Si NMR (79.4 MHz, C₆D₆): δ -0.8 (s, SiMe₂), -7.1 (s, SiMe₂), -85.2 (s, SiMe). ¹¹⁹Sn NMR (149.1 MHz, C₆D₆): δ -127.8 (s). Anal. Calcd for C₃₉H₆₀N₃RhSi₄Sn (904.9): C, 51.77; H, 6.68; N, 4.64. Found: C, 51.23; H, 6.99; N, 4.91.

[MeSi[SiMe₂N(p-tol)]₂[SiMe₂N(η⁶-p-tol)]SnRh(COD)] (3b). A 200 mg (0.27 mmol) portion of MeSi[SiMe₂N(p-tol)]₃SnLi(OEt)₂ (**2b**) and 67 mg (0.14 mmol) of [RhCl(COD)]₂ were suspended in precooled toluene at -78 °C. The orange suspension was stirred for 60 min in the cold before it was centrifuged. Then the centrifugate was concentrated in vacuo and stored at -30 °C to precipitate **3b** as a yellow solid (95 mg, 40%). FT-IR (KBr-disk): 3009 (w), 2944 (w), 2883 (w), 1603 (w), 1550 (w), 1497 (s), 1332 (m), 1247 (s), 1107 (w), 1031 (w), 917 (m), 809 (s), 778 (s), 677 (m), 508 (m) cm⁻¹. ¹H NMR (600.1 MHz, C₆D₆): δ 7.25 (d, ³*J*_{HH} = 8.2 Hz, 4H, tol), 7.10 - 7.00 (m, 4H, tol), 5.53 (d, ³*J*_{HH} = 7.2 Hz, 2H, η⁶-tol), 4.81 (d, ³*J*_{HH} = 7.3 Hz, 2H, η⁶-tol), 3.59 (s, br, 4H, CH₂COD), 2.25 (s, 6H, C₆H₄CH₃), 2.06 - 1.96 (m, 4H, CH₂ COD), 1.72 - 1.56 (m, 4H, CH₂ COD), 1.12 (s, 3H, η⁶-C₆H₄CH₃), 0.78 (s, 6H, Si(CH₃)₂), 0.62 (s, 6H, Si(CH₃)₂), 0.58 (s, 6H, Si(CH₃)₂), 0.35 (s, 3H, SiCH₃). ¹³C NMR (150.9 MHz, C₆D₆): δ 152.7 (s, C₁tol), 150.4 (s, br, C₁η⁶-tol), 129.6 (s, C_{3,5}tol), 129.4 (d, ¹*J*(¹⁰³Rh-¹³C) = 4.4 Hz, C_{3,5} η⁶-tol), 127.2 (s, C₄tol), 125.4 (s, C_{2,6}tol), 103.0 (d, ¹*J*(¹⁰³Rh-¹³C) = 4.4 Hz, C_{2,6} η⁶-tol), 93.2 (s, br, C₄ η⁶-tol), 78.4 (d, ¹*J*(¹⁰³Rh-¹³C) = 12.8 Hz, CH₂COD), 31.9 (s, CH₂ COD), 20.8 (s, C₆H₃CH₃), 17.4 (s, η⁶-C₆H₃CH₃), 4.1 (s, Si(CH₃)₂), 3.8 (s, Si(CH₃)₂), 2.9 (s, Si(CH₃)₂), -13.8 (s, SiCH₃). ²⁹Si NMR (39.7 MHz, C₆D₆): δ -1.2 (s, SiMe₂), -7.2 (s, SiMe₂), -85.4 (s, SiMe). ¹¹⁹Sn NMR (74.6 MHz, C₆D₆): δ -120.0 (s). Anal. Calcd for

(38) Giordano, G.; Crabtree, R. H. *Inorg. Synth.* **1990**, *28*, 88.

(39) Abel, E. W.; Bennett, M. A.; Wilkinson, G. *J. Chem. Soc.* **1959**, 3178.

(40) Cramer, R. *Inorg. Synth.* **1990**, *28*, 86.

(41) Herde, J. L.; Lambert, J. C.; Senoff, C. V. *Inorg. Synth.* **1974**, *15*, 18.

$C_{36}H_{54}N_3RhSi_4Sn$ (862.8): C, 50.11; H, 6.31; N, 4.87. Found: C, 49.34; H, 6.41; N, 4.66.

[MeSi[SiMe₂N(3,5-xy)]₃SnRh(PPh₃)(COD)] (4a). A mixture of 200 mg (0.26 mmol) of MeSi[SiMe₂N(3,5-xy)]₃SnLi(OEt₂) (**2a**) and 63 mg (0.13 mmol) of [RhCl(COD)]₂ was suspended in precooled toluene at -78 °C. The orange suspension was stirred for 15 min before a solution of 68 mg (0.259 mmol) of PPh₃ in cold toluene was added. After a further 15 min of cooling it was slowly warmed to room temperature and stirred for 2 h. Meanwhile the color changed to red, and then insolubilities were removed by centrifugation. The solvent was distilled in vacuo to get an orange powder (230 mg) in 76% yield. FT-IR (KBr-disk): 3020 (w), 2941 (w), 2915 (w), 2887 (w), 1597 (s), 1581 (s), 1476 (m), 1434 (m), 1295 (m), 1261 (m), 1241 (m), 1156 (m), 1092 (m), 1032 (m), 958 (m), 825 (s, br), 694 (m), 645 (m), 524 (w) cm⁻¹. ¹H NMR (399.9 MHz, C₆D₆): δ 7.39 (s, 4H, PPh₃), 7.10–6.97 (m, 17H, PPh₃), 2.6–*H*_{xy1}), 6.62 (s, 3H, 4-*H*_{xy1}), 5.95–5.86 (m, 2H, CH₂COD), 3.28–3.20 (m, 2H, CH₂COD), 2.28 (s, 18H, C₆H₃(CH₃)₂), 2.00–1.88 (m, 2H, CH₂COD), 1.74–1.63 (m, 2H, CH₂COD), 1.63–1.52 (m, 2H, CH₂COD), 1.25–1.13 (m, 2H, CH₂COD), 0.58 (s, 18H, Si(CH₃)₂), 0.27 (s, 3H, SiCH₃). ¹³C NMR (100.6 MHz, C₆D₆): δ 155.1 (s, 1-C_{xy1}), 137.5 (s, 3,5-C_{xy1}), 134.7 (d, $J(^{31}P-^{13}C)$ = 39 Hz, PPh₃), 134.4 (d, $J(^{31}P-^{13}C)$ = 12 Hz, PPh₃), 129.5 (d, $J(^{31}P-^{13}C)$ = 2.0 Hz, PPh₃), 127.9 (d, $J(^{31}P-^{13}C)$ = 9.7 Hz, PPh₃), 126.3 (s, 2,6-C_{xy1}), 125.7 (s, 4-C_{xy1}), 90.2 (d, $J(^{103}Rh-^{13}C)$ = 8.9 Hz, CH₂COD), 86.2 (t, $J(^{103}Rh-^{13}C)$ = 8.5 Hz, CH₂COD), 32.0 (s, CH₂COD), 29.1 (s, CH₂COD), 21.9 (s, C₆H₃(CH₃)₂), 5.0 (s, Si(CH₃)₂), -9.8 (s, SiCH₃). ²⁹Si NMR (79.4 MHz, C₆D₆): δ -2.9 (s, SiMe₂), -97.1 (s, SiMe). ³¹P NMR (161.9 MHz, C₆D₆): δ = 24.5 (d, $J(^{103}Rh-^{31}P)$ = 144 Hz, $J(^{117}Sn-^{31}P)$ = 334 Hz, $J(^{119}Sn-^{31}P)$ = 350 Hz), ¹¹⁹Sn NMR (149.1 MHz, C₆D₆): δ -176.0 (dd, $J(^{119}Sn-^{103}Rh)$ = 802 Hz, $J(^{119}Sn-^{31}P)$ = 349 Hz). Anal. Calcd for C₅₇H₇₅N₃PRhSi₄Sn (1167.2): C, 58.66; H, 6.48; N, 3.60. Found: C, 58.19; H, 6.78; N, 3.63.

[MeSi[SiMe₂N(p-tol)]₃SnRh(PPh₃)(COD)] (4b). A 500 mg (0.68 mmol) amount of MeSi[SiMe₂N(p-tol)]₃SnLi(OEt₂) (**2b**) and 168 mg (0.34 mmol) of [RhCl(COD)]₂ were suspended at -78 °C with precooled Et₂O. After 30 min the orange reaction mixture was filtered and added to solid PPh₃ (178 mg, 0.68 mmol). The solution was slowly warmed to room temperature after 1.5 h and the solvent was removed in vacuo. The orange residue was washed twice with small amounts of pentane and dried under reduced pressure to yield the product (613 mg, 80% yield) as an orange powder. A concentrated solution of **4b** in Et₂O was stored at -30 °C to give orange crystals. FT-IR (KBr-disk): 3054 (w), 3012 (w), 2940 (m), 2890 (m), 1604 (w), 1498 (s), 1433 (w), 1222 (s), 1092 (w), 908 (s), 938 (m), 814 (m), 777 (m), 698 (w), 510 (m) cm⁻¹. ¹H NMR (200 MHz, C₆D₆): δ 7.26–7.18 (m, 9H, tol, PPh₃ overlap), 7.08–6.98 (m, 12H, PPh₃), 6.89 (d, J_{HH} = 7.9 Hz, 6H, tol), 5.82 (s, br, 2H, CH₂COD), 3.36 (s, br, 2H, CH₂COD), 2.24 (s, 9H, C₆H₄CH₃), 1.80 (s, br, 2H, CH₂COD), 1.53 (s, br, 4H, CH₂COD), 1.20 (s, br, 2H, CH₂COD), 0.57 (s, 18H, Si(CH₃)₂), 0.36 (s, 3H, SiCH₃). ¹³C NMR (50.3 MHz, C₆D₆): δ 151.9 (s, tol), 134.6 (d, $J(^{31}P-^{13}C)$ = 12 Hz, PPh₃), 134.2 (d, $J(^{31}P-^{13}C)$ = 40 Hz, PPh₃), 129.8 (s, tol), 129.7 (d, $J(^{31}P-^{13}C)$ = 13 Hz, PPh₃), 129.5 (s, tol), 128.9 (s, tol), 127.5 (s, PPh₃), 91.1 (d, $J(^{103}Rh-^{13}C)$ = 12 Hz, CH₂COD), 87.1 (d, $J(^{103}Rh-^{13}C)$ = 12 Hz, CH₂COD), 31.4 (s, br, CH₂COD), 29.5 (s, br, CH₂COD), 20.7 (s, C₆H₄CH₃), 4.3 (s, Si(CH₃)₂), -14.3 (s, SiCH₃). ²⁹Si NMR (39.7 MHz, C₆D₆): δ -2.3 (s, SiMe₂), -91.8 (s, SiMe). ³¹P NMR (80.9 MHz, C₆D₆): δ = 29.4 (d, $J(^{103}Rh-^{31}P)$ = 148 Hz, $J(^{117}Sn-^{31}P)$ = 296 Hz, $J(^{119}Sn-^{31}P)$ = 309 Hz), ¹¹⁹Sn NMR (149.1 MHz, C₆D₆): δ -176.5 (dd, $J(^{119}Sn-^{103}Rh)$ = 806 Hz, $J(^{119}Sn-^{31}P)$ = 311 Hz). Anal. Calcd for C₅₄H₆₉N₃PRhSi₄Sn (1125.1): C, 57.65; H, 6.18; N, 3.73. Found: C, 57.83; H, 6.32; N, 3.58.

[MeSi[SiMe₂N(3,5-xy)]₃SnRh(PPh₃)(NBD)] (5a). The reaction procedure was the same as for **4a** using 200 mg (0.26 mmol) of MeSi[SiMe₂N(3,5-xy)]₃SnLi(OEt₂) (**2a**), 59 mg (0.13 mmol) of [RhCl(NBD)]₂, and 68 mg (0.26 mmol) of PPh₃. Compound **5a**

was isolated as a bright orange microcrystalline solid in 83% (248 mg) yield. The product could be crystallized from a solution in toluene at -30 °C. FT-IR (KBr-disk): 3002 (w), 2942 (w), 2858 (w), 1596 (m), 1581 (s), 1477 (w), 1434 (m), 1351 (w), 1298 (s), 1239 (m), 1157 (m), 1091 (w), 1036 (m), 961 (m), 890 (m), 856 (s), 828 (s), 779 (m), 747 (m), 699 (s), 646 (m), 509 (m) cm⁻¹. ¹H NMR (399.9 MHz, C₆D₆): δ 7.41–7.34 (m, 8H, PPh₃), 7.07–6.97 (m, 25H, PPh₃), 6.96 (s, 6H, 2,6-*H*_{xy1}), 6.60 (s, 3H, 4-*H*_{xy1}), 5.35–4.85 (m, 2H, 2/3/5/6-NBD CH), 3.16 (s, br, 2H, 1/4-NBD CH), 3.02–2.66 (m, 2H, 2/3/5/6-NBD CH), 2.29 (s, 18H, C₆H₃(CH₃)₂), 1.42–1.26 (m, 2H, CH₂NBD), 0.62 (s, 18H, Si(CH₃)₂), 0.28 (s, 3H, SiCH₃). ¹³C NMR (150.9 MHz, C₆D₆): δ 155.3 (s, 1-C_{xy1}), 137.6 (s, 3,5-C_{xy1}), 134.2 (d, $J(^{31}P-^{13}C)$ = 20 Hz, PPh₃), 134.0 (d, $J(^{31}P-^{13}C)$ = 12 Hz, PPh₃), 133.5 (d, $J(^{31}P-^{13}C)$ = 39 Hz, PPh₃), 128.9 (d, $J(^{31}P-^{13}C)$ = 9.5 Hz, PPh₃), 125.3 (s, 2,6-C_{xy1}), 122.4 (s, 4-C_{xy1}), 70.1 (s, br, 2/3/5/6-NBD CH), 66.7 (s, CH₂NBD), 52.1 (s, 1/4-NBD CH), 21.9 (s, C₆H₃(CH₃)₂), 4.7 (s, Si(CH₃)₂), -14.6 (s, SiCH₃). ²⁹Si NMR (79.4 MHz, C₆D₆): δ -3.2 (s, SiMe₂), -96.3 (s, SiMe). ³¹P NMR (161.9 MHz, C₆D₆): δ 32.0 (d, $J(^{103}Rh-^{31}P)$ = 156 Hz, $J(^{117}Sn-^{31}P)$ = 331 Hz, $J(^{119}Sn-^{31}P)$ = 348 Hz), ¹¹⁹Sn NMR (74.6 MHz, C₆D₆): δ -146.4 (dd, $J(^{119}Sn-^{103}Rh)$ = 910 Hz, $J(^{119}Sn-^{31}P)$ = 349 Hz). Anal. Calcd for C₅₆H₇₁N₃PRhSi₄Sn x C₆H₅CH₃ (1151.1): C, 59.69; H, 6.31; N, 3.51. Found: C, 59.68; H, 6.65; N, 3.64.

[MeSi[SiMe₂N(p-tol)]₃SnRh(PPh₃)(NBD)] (5b). The reaction procedure was the same as for **4b** using 502 mg (0.69 mmol) of MeSi[SiMe₂N(p-tol)]₃SnLi(OEt₂) (**2b**), 159 mg (0.35 mmol) of [RhCl(NBD)]₂, and 181 mg (0.69 mmol) of PPh₃. Compound **5b** was isolated as a bright orange microcrystalline solid in 79% (604 mg) yield. Crystallization from a saturated solution in pentane at -30 °C gave suitable crystals for X-ray analysis. FT-IR (KBr-disk): 3053 (w), 3011 (w), 2956 (w), 2891 (w), 1605 (w), 1497 (s), 1434 (m), 1236 (s), 1223 (s), 1091 (w), 914 (s), 844 (m), 813 (m), 778 (m), 744 (m), 698 (m), 543 (w), 528 (w), 509 (m) cm⁻¹. ¹H NMR (199.9 MHz, C₆D₆): δ 7.20 (d, J_{HH} = 8.1 Hz, 6H, tol), 7.12–6.96 (m, 15H, PPh₃), 6.84 (d, J_{HH} = 8.0 Hz, 6H, tol), 4.00 (s, br, 4H, 2/3/5/6-NBD CH), 3.09 (s, br, 2H, 1/4-NBD CH), 2.18 (s, 9H, C₆H₄CH₃), 0.82 (s, br, 2H, CH₂NBD), 0.64 (s, 18H, Si(CH₃)₂), 0.30 (s, 3H, SiCH₃). ¹³C NMR (50.3 MHz, C₆D₆): δ 152.3 (s, tol), 133.9 (d, $J(^{31}P-^{13}C)$ = 12 Hz, PPh₃), 132.8 (d, $J(^{31}P-^{13}C)$ = 40 Hz, PPh₃), 129.6 (d, $J(^{31}P-^{13}C)$ = 20 Hz, PPh₃), 129.1 (s, tol), 128.0 (s, PPh₃), 127.9 (s, tol), 125.5 (s, tol), 69.2 (s, br, 2/3/5/6-NBD CH), 65.6 (s, CH₂NBD), 51.5 (s, 1/4-NBD CH), 20.6 (s, C₆H₄CH₃), 4.2 (s, Si(CH₃)₂), -14.4 (s, SiCH₃). ²⁹Si NMR (39.7 MHz, C₆D₆): δ -2.4 (s, SiMe₂), -91.1 (s, SiMe). ³¹P NMR (80.9 MHz, C₆D₆): δ = 33.5 (d, $J(^{103}Rh-^{31}P)$ = 159 Hz, $J(^{117}Sn-^{31}P)$ = 305 Hz, $J(^{119}Sn-^{31}P)$ = 319 Hz), ¹¹⁹Sn NMR (74.6 MHz, C₆D₆): δ -147.7 (dd, $J(^{119}Sn-^{103}Rh)$ = 910 Hz, $J(^{119}Sn-^{31}P)$ = 315 Hz). Anal. Calcd for C₅₃H₆₅N₃PRhSi₄Sn (1109.0): C, 57.40; H, 5.91; N, 3.79. Found: C, 57.24; H, 6.06; N, 3.78.

[MeSi[SiMe₂N(3,5-xy)]₃SnRh(PPh₃)(η^6 -C₆H₆)] (6a). A solution of 68 mg (0.26 mmol) of PPh₃ in pentane and 2 mL of benzene was cooled to -78 °C. In the cold it was added to a solid mixture of 200 mg (0.26 mmol) of MeSi[SiMe₂N(3,5-xy)]₃SnLi(OEt₂) (**2a**) and 50 mg (0.13 mmol) of [RhCl(C₂H₄)₂]₂. The yellow suspension was stirred for 15 min. Then it was allowed to warm to room temperature, while a color change to brown occurred. Insolubilities were removed by centrifugation and solvents in vacuo to yield 258 mg (87%) of a brown powder. FT-IR (Nujol): 3033 (w), 2946 (m), 2893 (m), 2859 (w), 1596 (m), 1583 (s), 1478 (m), 1458 (m), 1436 (m), 1352 (w), 850 (m), 830 (m), 781 (m), 746 (m), 701 (m), 647 (m), 598 (m) cm⁻¹. ¹H NMR (400 MHz, C₆D₆): δ 7.01–6.98 (m, 6H, PPh₃), 6.96 (s, 6H, η^6 -C₆H₆), 6.96–6.92 (m, 9H, PPh₃), 6.92 (s, 6H, 2,6-*H*_{xy1}), 6.65 (s, 3H, 4-*H*_{xy1}), 2.29 (s, 18H, C₆H₃(CH₃)₂), 0.57 (s, 18H, Si(CH₃)₂), 0.28 (s, 3H, SiCH₃). ¹H NMR (400 MHz, C₆D₁₂): δ 7.15–7.08 (m, 3H, PPh₃), 7.07–7.00 (m, 6H, PPh₃), 6.87–6.76 (m, 6H, PPh₃), 6.60 (s, 6H, 2,6-*H*_{xy1}), 6.54 (s, 3H, 4-*H*_{xy1}),

Table 1. Details of the Crystal Structure Determinations of 2a, 3a, 4b, 5a, 4b, 5a, 5b, 6b, and 8b

	2a	3a	4b	5a	5b	6b	8b
formula	C ₃₅ H ₅₈ LiN ₃ OSi ₄	C ₃₉ H ₆₀ N ₃ RhSi ₄ Sn	C ₅₃ H ₆₉ N ₃ PRhSi ₄ Sn	C ₇₄ H ₈₉ N ₃ PRhSi ₄ Sn	C ₃₅ H ₆₅ N ₃ PRhSi ₄ Sn	C ₅₃ H ₆₆ N ₃ PRhSi ₄ Sn	C ₅₄ H ₆₉ IrN ₃ PSi ₄ Sn
cryst syst	triclinic	monoclinic	monoclinic	triclinic	orthorhombic	triclinic	monoclinic
space group	<i>P</i> $\bar{1}$	<i>P</i> ₂ / <i>c</i>	<i>P</i> ₂ / <i>n</i>	<i>P</i> $\bar{1}$	<i>Pbcn</i>	<i>P</i> $\bar{1}$	<i>P</i> ₂ / <i>c</i>
<i>a</i> /Å	12.5582(9)	14.2713(16)	14.1402(17)	12.9830(13)	42.049(4)	11.870(3)	12.910(5)
<i>b</i> /Å	13.3633(10)	12.3970(15)	23.380(3)	13.2225(13)	12.9598(11)	11.947(2)	16.198(8)
<i>c</i> /Å	16.1012(12)	25.911(3)	15.953(2)	21.979(2)	19.6423(17)	19.451(5)	28.002(9)
α /deg	71.821(2)			95.447(2)		85.419(5)	
β /deg	67.9890(10)	102.079(3)	96.568(2)	105.608(2)		81.054(4)	115.862(19)
γ /deg	65.6830(10)			104.915(2)		81.686(4)	
<i>V</i> /Å ³	2242.8(3)	4482.7(9)	5239.4(11)	3456.4(6)	10704.0(16)	2691.5(11)	5269(4)
Z	2	4	4	2	8	2	4
<i>M_r</i>	774.83	904.86	1125.05	1385.41	1109.01	1134.04	1214.34
<i>d_c</i> /Mg m ⁻³	1.150	1.340	1.430	1.330	1.380	1.400	1.531
<i>F</i> ₀₀₀	812	1864	2320	1440	4560	1166	2448
μ (Mo K α)/mm ⁻¹	0.700	1.060	0.950	0.740	0.930	0.930	3.157
max., min. transmission factors	0.8702, 0.8239	0.7463, 0.5273	0.7452, 0.6366	0.9750, 0.8568	0.9126, 0.8106	0.9130, 0.7665	0.7522, 0.7231
X-radiation, λ /Å				Mo K α , graphite monochromated, 0.71073			
data collect. temp/K	100(2)	100(2)	100(2)	100(2)	100(2)	193(2)	100(2)
θ range/deg	1.7 to 30.0	1.9 to 25.7	2.0 to 25.0	2.0 to 27.5	1.6 to 25.0	1.1 to 27.0	1.5 to 30.5
index ranges, <i>h, k, l</i>	-16 ... 17, -17 ... 18, 0 ... 22	-17 ... 17, 0 ... 15, 0 ... 31	-16 ... 16, 0 ... 27, 0 ... 18	-16 ... 16, -17 ... 17, 0 ... 28	0 ... 50, 0 ... 15, 0 ... 23	-14 ... 15, -15 ... 15, 0 ... 24	-18 ... 18, -23 ... 0, -40 ... 17
reflms measd	53 215	76 870	87 929	68 634	63 386	22 085	16 586
unique, <i>R</i> _{int}	13 103, 0.0562	8472, 0.1125	9251, 0.1235	15 828, 0.0931	9454, 0.1168	11 619, 0.0372	16 062, 0.0410
obsd [<i>I</i> \geq 2 σ (<i>I</i>)]	10420	5519	6360	10049	6515	9017	12749
params refined	420	446	599	782	578	596	603
<i>R</i> indices (all data)	<i>R</i> 1 = 0.0359, <i>wR</i> 2 = 0.0841	<i>R</i> 1 = 0.0551, <i>wR</i> 2 = 0.1310	<i>R</i> 1 = 0.0492, <i>wR</i> 2 = 0.1127	<i>R</i> 1 = 0.0501, <i>wR</i> 2 = 0.1120	<i>R</i> 1 = 0.0554, <i>wR</i> 2 = 0.1259	<i>R</i> 1 = 0.0376, <i>wR</i> 2 = 0.0692	<i>R</i> 1 = 0.0348, <i>wR</i> 2 = 0.0795
<i>R</i> indices [<i>I</i> > 2 σ (<i>I</i>)]	<i>R</i> 1 = 0.0501, <i>wR</i> 2 = 0.0894	<i>R</i> 1 = 0.0849, <i>wR</i> 2 = 0.1467	<i>R</i> 1 = 0.0766, <i>wR</i> 2 = 0.1254	<i>R</i> 1 = 0.0925, <i>wR</i> 2 = 0.1272	<i>R</i> 1 = 0.0844, <i>wR</i> 2 = 0.1366	<i>R</i> 1 = 0.0580, <i>wR</i> 2 = 0.0744	<i>R</i> 1 = 0.0486, <i>wR</i> 2 = 0.0853
Good on <i>F</i> ²	1.112	0.991	0.991	0.990	1.022	1.048	1.09
largest residual peaks /e Å ⁻³	0.917 and -0.575	0.861, -1.490	0.650, -0.928	1.382, -1.115	1.197, -1.414	0.445, -0.393	2.978, -1.041

5.19 (s, 6H, $\eta^6\text{-C}_6\text{H}_6$), 2.23 (s, 18H, $\text{C}_6\text{H}_3(\text{CH}_3)_2$), 0.18 (s, 18H, $\text{Si}(\text{CH}_3)_2$), 0.06 (s, 3H, SiCH_3). ^{13}C NMR (100.6 MHz, C_6D_6): δ 154.3 (s, 1- C_{xyli}), 139.6 (d, $J(^{31}\text{P}-^{13}\text{C}) = 46$ Hz, PPh_3), 137.1 (s, 3,5- C_{xyli}), 133.7 (d, $J(^{31}\text{P}-^{13}\text{C}) = 13$ Hz, PPh_3), 129.0 (d, $J(^{31}\text{P}-^{13}\text{C}) = 2.1$ Hz, PPh_3), 128.6 (s, $\eta^6\text{-C}_6\text{H}_6$), 127.8 (s, 2,6- C_{xyli}), 127.5 (d, $J(^{31}\text{P}-^{13}\text{C}) = 10$ Hz, PPh_3), 122.5 (s, 4- C_{xyli}), 21.9 (s, $\text{C}_6\text{H}_3(\text{CH}_3)_2$), 5.0 (s, $\text{Si}(\text{CH}_3)_2$), -14.6 (s, SiCH_3). ^{29}Si NMR (79.4 MHz, C_6D_6): δ -2.7 (s, SiMe_2), -97.4 (s, SiMe). ^{13}C NMR (100.6 MHz, C_6D_6): δ = 153.6 (s, 1- C_{xyli}), 139.1 (d, $J(^{31}\text{P}-^{13}\text{C}) = 44$ Hz, PPh_3), 136.2 (s, 3,5- C_{xyli}), 133.3 (d, $J(^{31}\text{P}-^{13}\text{C}) = 12$ Hz, PPh_3), 128.1 (s, PPh_3), 127.3 (s, 2,6- C_{xyli}), 126.7 (d, $J(^{31}\text{P}-^{13}\text{C}) = 10$ Hz, PPh_3), 121.7 (s, 4- C_{xyli}), 96.3 (s, $\eta^6\text{-C}_6\text{H}_6$), 21.0 (s, $\text{C}_6\text{H}_3(\text{CH}_3)_2$), 3.7 (s, $\text{Si}(\text{CH}_3)_2$), -15.7 (s, SiCH_3). ^{31}P NMR (161.9 MHz, C_6D_6): δ 39.9 (d, $^1J(^{103}\text{Rh}-^{31}\text{P}) = 214$ Hz, $^2J(^{117}\text{Sn}-^{31}\text{P}) = 343$ Hz, $^2J(^{119}\text{Sn}-^{31}\text{P}) = 358$ Hz). ^{119}Sn NMR (149.1 MHz, C_6D_6): δ -175.5 (dd, $^1J(^{119}\text{Sn}-^{103}\text{Rh}) = 1159$ Hz, $^2J(^{119}\text{Sn}-^{31}\text{P}) = 360$ Hz). Anal. Calcd for $\text{C}_{55}\text{H}_{69}\text{N}_3\text{PRhSi}_4\text{Sn}$ (1137.1): C, 58.09; H, 6.12; N, 3.70. Found: C, 57.76; H, 6.49; N, 3.75.

[MeSi[SiMe₂N(p-tol)]₃SnRh(PPh₃)($\eta^6\text{-C}_6\text{H}_6$)] (6b). An analogous procedure as for preparing **6a**, using 200 mg (0.27 mmol) of MeSi[SiMe₂N(p-tol)]₃SnLi(OEt₂) (**2b**), 53 mg (0.14 mmol) of [RhCl(C₂H₄)₂]₂, and 72 mg of PPh₃ (0.27 mmol), gave compound **6b** as a brown microcrystalline solid in yield 41% (124 mg). FT-IR (KBr-disk): 3054 (w), 2958 (m), 1615 (w), 1512 (s), 1499 (s), 1436 (s), 1286 (m), 1261 (s), 1120 (m), 1093 (s), 1027 (m), 909 (m), 812 (s), 747 (w), 694 (s), 541 (m) cm⁻¹. ^1H NMR (400 MHz, C_6D_6): δ 7.82–7.69 (m, 4H, PPh_3), 7.10 (d, $^3J_{\text{HH}} = 8.2$ Hz, 6H, tol), 7.07–7.01 (m, 9H, PPh_3), 6.99 (s, 6H, $\eta^6\text{-C}_6\text{H}_6$), 6.93 (d, $^3J_{\text{HH}} = 8.2$ Hz, 6H, tol), 6.90–6.79 (m, 2H, PPh_3), 2.30 (s, 9H, $\text{C}_6\text{H}_4\text{CH}_3$), 0.55 (s, 18H, $\text{Si}(\text{CH}_3)_2$), 0.26 (s, 3H, SiCH_3). ^1H NMR (600 MHz, C_6D_6): δ 7.16–7.00 (m, 9H, PPh_3), 6.95–6.81 (m, 6H, PPh_3), 6.86 (d, $^3J_{\text{HH}} = 3.6$ Hz, 6H, tol), 6.84 (d, $^3J_{\text{HH}} = 3.5$ Hz, 6H, tol), 5.21 (s, 6H, $\eta^6\text{-C}_6\text{H}_6$), 2.33 (s, 9H, $\text{C}_6\text{H}_4\text{CH}_3$), 0.23 (s, 18H, $\text{Si}(\text{CH}_3)_2$), 0.11 (s, 3H, SiCH_3). ^{13}C NMR (100.6 MHz, C_6D_6): δ 151.6 (s, 1- C_{toi}), 134.1 (d, $J(^{31}\text{P}-^{13}\text{C}) = 12$ Hz, PPh_3), 129.0 (d, $J(^{31}\text{P}-^{13}\text{C}) = 4.6$ Hz, PPh_3), 128.6 (d, $J(^{31}\text{P}-^{13}\text{C}) = 8.4$ Hz, PPh_3), 127.5 (d, $J(^{31}\text{P}-^{13}\text{C}) = 10$ Hz, PPh_3), 21.1 (s, $\text{C}_6\text{H}_3(\text{CH}_3)_2$), 4.8 (s, $\text{Si}(\text{CH}_3)_2$), -14.2 (s, SiCH_3). ^{13}C NMR (100.6 MHz, C_6D_6): δ 151.0 (s, 1- C_{toi}), 140.2 (d, $J(^{31}\text{P}-^{13}\text{C}) = 52$ Hz, PPh_3), 133.6 (d, $J(^{31}\text{P}-^{13}\text{C}) = 12$ Hz, PPh_3), 128.6 (s, 3,5- C_{toi}), 128.2 (s, PPh_3), 127.7 (s, 2,6- C_{toi}), 126.7 (d, $J(^{31}\text{P}-^{13}\text{C}) = 10$ Hz, PPh_3), 124.9 (s, 4- C_{xyli}), 96.6 (s, $\eta^6\text{-C}_6\text{H}_6$), 20.3 (s, $\text{C}_6\text{H}_4\text{CH}_3$), 3.7 (s, $\text{Si}(\text{CH}_3)_2$), -15.5 (s, SiCH_3). ^{29}Si NMR (79.4 MHz, C_6D_6): δ -2.6 (s, SiMe_2), -93.7 (s, SiMe). ^{31}P NMR (161.9 MHz, C_6D_6): δ 42.8 (d, $^1J(^{103}\text{Rh}-^{31}\text{P}) = 215$ Hz, $^2J(^{117}\text{Sn}-^{31}\text{P}) = 322$ Hz, $^2J(^{119}\text{Sn}-^{31}\text{P}) = 343$ Hz). ^{119}Sn NMR (149.1 MHz, C_6D_6): δ -179.7 (dd, $^1J(^{119}\text{Sn}-^{103}\text{Rh}) = 1170$ Hz, $^2J(^{119}\text{Sn}-^{31}\text{P}) = 337$ Hz). Anal. Calcd for $\text{C}_{52}\text{H}_{63}\text{N}_3\text{PRhSi}_4\text{Sn}$ (1095.0): C, 57.04; H, 5.80; N, 3.84. Found: C, 56.80; H, 5.89; N, 4.02.

[MeSi[SiMe₂N(3,5-xyl)]₃SnRh(PPh₃)($\eta^6\text{-C}_6\text{H}_5\text{CH}_3$)] (7a). A solution of 68 mg (0.26 mmol) of PPh₃ in pentane and 5 mL of toluene was cooled to -78 °C. In the cold it was added to a solid mixture of 200 mg (0.26 mmol) of MeSi[SiMe₂N(3,5-xyl)]₃SnLi(OEt₂) (**2a**) and 50 mg (0.13 mmol) of [RhCl(C₂H₄)₂]₂. The yellow suspension was stirred for 15 min and then allowed to warm to room temperature. During the course of this procedure, a change of color of the reaction mixture from yellow to brown was observed. Insolubilities were removed by centrifugation and solvents in vacuo to yield 203 mg (68%) of a brown powder. FT-IR (KBr-disk): 3022 (w), 2954 (w), 2914 (w), 2858 (w), 1595 (s), 1582 (s), 1477 (m), 1435 (m), 1351 (w), 1294 (m), 1241 (m), 1156 (s), 1092 (m), 1030 (m), 956 (m), 908 (s), 854 (s), 775 (s), 703 (s), 644 (m), 530 (m) cm⁻¹. ^1H NMR (400 MHz, C_6D_6): δ 7.13–7.09 (m, 1H, $\eta^6\text{-C}_6\text{H}_5\text{CH}_3$), 7.06–7.02 (m, 1H, PPh_3), 7.02–6.98 (m, 4H, $\eta^6\text{-C}_6\text{H}_5\text{CH}_3$), 6.98–6.92 (m, 14H, PPh_3), 6.91 (s, 6H, 2,6- H_{xyli}), 6.65 (s, 3H, 4- H_{xyli}), 2.29 (s, 18H, $\text{C}_6\text{H}_3(\text{CH}_3)_2$), 2.10 (s, 3H, $\eta^6\text{-C}_6\text{H}_5\text{CH}_3$), 0.57 (s, 18H, $\text{Si}(\text{CH}_3)_2$), 0.27 (s, 3H, SiCH_3). ^1H NMR

(400 MHz, C_6D_6): δ 7.14–7.01 (m, 9H, PPh_3), 6.90–6.82 (m, 6H, PPh_3), 6.58 (s, 6H, 2,6- H_{xyli}), 6.54 (s, 3H, 4- H_{xyli}), 6.10–6.05 (m, 1H, $\eta^6\text{-C}_6\text{H}_5\text{CH}_3$), 5.07 (t, 2H, $^3J_{\text{HH}} = 6.2$ Hz, $\eta^6\text{-C}_6\text{H}_5\text{CH}_3$), 4.28 (d, 2H, $^3J_{\text{HH}} = 6.2$ Hz, $\eta^6\text{-C}_6\text{H}_5\text{CH}_3$), 2.23 (s, 18H, $\text{C}_6\text{H}_3(\text{CH}_3)_2$), 1.71 (s, 3H, $\eta^6\text{-C}_6\text{H}_5\text{CH}_3$), 0.18 (s, 18H, $\text{Si}(\text{CH}_3)_2$), 0.07 (s, 3H, SiCH_3). ^{13}C NMR (100.6 MHz, C_6D_6): δ 154.2 (s, 1- C_{xyli}), 139.1 (d, $J(^{31}\text{P}-^{13}\text{C}) = 46$ Hz, PPh_3), 137.1 (s, 3,5- C_{xyli}), 133.7 (d, $J(^{31}\text{P}-^{13}\text{C}) = 12$ Hz, PPh_3), 129.3 (s, $\eta^6\text{-C}_6\text{H}_5\text{CH}_3$), 128.9 (d, $J(^{31}\text{P}-^{13}\text{C}) = 2.3$ Hz, PPh_3), 128.5 (s, $\eta^6\text{-C}_6\text{H}_5\text{CH}_3$), 128.3 (s, $\eta^6\text{-C}_6\text{H}_5\text{CH}_3$), 127.7 (s, 2,6- C_{xyli}), 127.4 (d, $J(^{31}\text{P}-^{13}\text{C}) = 10$ Hz, PPh_3), 125.6 (s, $\eta^6\text{-C}_6\text{H}_5\text{CH}_3$), 122.5 (s, 4- C_{xyli}), 21.8 (s, $\text{C}_6\text{H}_3(\text{CH}_3)_2$), 21.4 (s, $\eta^6\text{-C}_6\text{H}_5\text{CH}_3$), 4.9 (s, $\text{Si}(\text{CH}_3)_2$), -14.7 (s, SiCH_3). ^{13}C NMR (100.6 MHz, C_6D_6): δ 153.8 (s, 1- C_{xyli}), 136.2 (s, 3,5- C_{xyli}), 133.1 (d, $J(^{31}\text{P}-^{13}\text{C}) = 13$ Hz, PPh_3), 128.0 (s, br, PPh_3), 127.3 (s, 2,6- C_{xyli}), 126.8 (d, $J(^{31}\text{P}-^{13}\text{C}) = 10$ Hz, PPh_3), 121.8 (s, 4- C_{xyli}), 98.1 (s, $\eta^6\text{-C}_6\text{H}_5\text{CH}_3$), 97.7 (s, $\eta^6\text{-C}_6\text{H}_5\text{CH}_3$), 93.0 (s, $\eta^6\text{-C}_6\text{H}_5\text{CH}_3$), 21.0 (s, $\text{C}_6\text{H}_3(\text{CH}_3)_2$), 19.4 (s, $\eta^6\text{-C}_6\text{H}_5\text{CH}_3$), 3.7 (s, $\text{Si}(\text{CH}_3)_2$), -15.7 (s, SiCH_3). ^{29}Si NMR (79.4 MHz, C_6D_6): δ -2.7 (s, SiMe_2), -97.4 (s, SiMe). ^{31}P NMR (161.9 MHz, C_6D_6): δ 39.9 (d, $^1J(^{103}\text{Rh}-^{31}\text{P}) = 215$ Hz, $^2J(^{117}\text{Sn}-^{31}\text{P}) = 343$ Hz, $^2J(^{119}\text{Sn}-^{31}\text{P}) = 358$ Hz). ^{119}Sn NMR (149.1 MHz, C_6D_6): δ -175.4 (dd, $^1J(^{119}\text{Sn}-^{103}\text{Rh}) = 1165$ Hz, $^2J(^{119}\text{Sn}-^{31}\text{P}) = 358$ Hz). Anal. Calcd for $\text{C}_{56}\text{H}_{71}\text{N}_3\text{PRhSi}_4\text{Sn}$ (1151.1): C, 58.43; H, 6.22; N, 3.65. Found: C, 58.16; H, 6.37; N, 3.64.

[MeSi[SiMe₂N(p-tol)]₃SnRh(PPh₃)($\eta^6\text{-C}_6\text{H}_5\text{CH}_3$)] (7b). An analogous procedure as that described for the preparation of **7a**, using 200 mg (0.27 mmol) of MeSi[SiMe₂N(p-tol)]₃SnLi(OEt₂) (**2b**), 53 mg (0.14 mmol) of [RhCl(C₂H₄)₂]₂, and 72 mg (0.27 mmol) of PPh₃, gave compound **7a** as a brown microcrystalline solid in 58% (176 mg) yield. FT-IR (KBr-disk): 3050 (w), 3015 (w), 2938 (w), 2890 (w), 1603 (m), 1498 (s), 1435 (m), 1232 (s), 1223 (s), 1092 (m), 1028 (w), 906 (s), 849 (m), 778 (m), 745 (m), 696 (s), 530 (m) cm⁻¹. ^1H NMR (400 MHz, C_6D_6): δ 7.13–6.96 (m, 15H, PPh_3 , 6H, tol, 5H, $\eta^6\text{-C}_6\text{H}_5\text{CH}_3$), 6.93 (d, $^3J_{\text{HH}} = 8.1$ Hz, 6H, tol), 2.30 (s, 9H, $\text{C}_6\text{H}_4\text{CH}_3$), 2.10 (s, 3H, $\eta^6\text{-C}_6\text{H}_5\text{CH}_3$), 0.56 (s, 18H, $\text{Si}(\text{CH}_3)_2$), 0.27 (s, 3H, SiCH_3). ^1H NMR (600 MHz, C_6D_6): δ 7.12–7.04 (m, 9H, PPh_3), 7.00–6.95 (m, 6H, PPh_3), 6.85 (d, $^3J_{\text{HH}} = 8.4$ Hz, 6H, tol), 6.83 (d, $^3J_{\text{HH}} = 8.4$ Hz, 6H, tol), 6.00 (t, 1H, $^3J_{\text{HH}} = 6.1$ Hz, $\eta^6\text{-C}_6\text{H}_5\text{CH}_3$), 5.09 (t, 2H, $^3J_{\text{HH}} = 6.2$ Hz, $\eta^6\text{-C}_6\text{H}_5\text{CH}_3$), 4.22 (d, 2H, $^3J_{\text{HH}} = 6.2$ Hz, $\eta^6\text{-C}_6\text{H}_5\text{CH}_3$), 2.32 (s, 9H, $\text{C}_6\text{H}_4\text{CH}_3$), 1.83 (s, 3H, $\eta^6\text{-C}_6\text{H}_5\text{CH}_3$), 0.22 (s, 18H, $\text{Si}(\text{CH}_3)_2$), 0.10 (s, 3H, SiCH_3). ^{13}C NMR (100 MHz, C_6D_6): δ 151.6 (s, 1- C_{toi}), 139.4 (d, $J(^{31}\text{P}-^{13}\text{C}) = 45$ Hz, PPh_3), 137.9 (s, $\eta^6\text{-C}_6\text{H}_5\text{CH}_3$), 134.1 (d, $J(^{31}\text{P}-^{13}\text{C}) = 13$ Hz, PPh_3), 129.3 (s, 3,5- C_{toi}), 129.2 (s, $\eta^6\text{-C}_6\text{H}_5\text{CH}_3$), 129.0 (d, $J(^{31}\text{P}-^{13}\text{C}) = 3.5$ Hz, PPh_3), 128.7 (s, $\eta^6\text{-C}_6\text{H}_5\text{CH}_3$), 128.6 (s, 2,6- C_{toi}), 128.3 (s, $\eta^6\text{-C}_6\text{H}_5\text{CH}_3$), 127.5 (d, $J(^{31}\text{P}-^{13}\text{C}) = 10$ Hz, PPh_3), 125.7 (s, 4- C_{toi}), 21.4 (s, $\eta^6\text{-CH}_3\text{C}_6\text{H}_5$), 21.1 (s, $\text{C}_6\text{H}_3(\text{CH}_3)_2$), 4.8 (s, $\text{Si}(\text{CH}_3)_2$), -14.2 (s, SiCH_3). ^{13}C NMR (150.9 MHz, C_6D_6): δ 151.2 (s, 1- C_{toi}), 136.9 (s, 4- C_{toi}), 133.5 (d, $J(^{31}\text{P}-^{13}\text{C}) = 13$ Hz, PPh_3), 129.3 (s, 3,5- C_{toi}), 128.7 (s, 2,6- C_{toi}), 128.2 (s, br, PPh_3), 128.0 (d, $J(^{31}\text{P}-^{13}\text{C}) = 31$ Hz, PPh_3), 126.7 (d, $J(^{31}\text{P}-^{13}\text{C}) = 10$ Hz, PPh_3), 100.1 (s, $\eta^6\text{-C}_6\text{H}_5\text{CH}_3$), 97.1 (s, $\eta^6\text{-C}_6\text{H}_5\text{CH}_3$), 92.4 (s, $\eta^6\text{-C}_6\text{H}_5\text{CH}_3$), 20.2 (s, $\text{C}_6\text{H}_3(\text{CH}_3)_2$), 18.6 (s, $\eta^6\text{-CH}_3\text{C}_6\text{H}_5$), 3.6 (s, $\text{Si}(\text{CH}_3)_2$), -15.5 (s, SiCH_3). ^{29}Si NMR (79.4 MHz, C_6D_6): δ -2.1 (s, SiMe_2), -93.7 (s, SiMe). ^{31}P NMR (242.9 MHz, C_6D_6): δ 42.9 (d, $^1J(^{103}\text{Rh}-^{31}\text{P}) = 215$ Hz, $^2J(^{117}\text{Sn}-^{31}\text{P}) = 323$ Hz, $^2J(^{119}\text{Sn}-^{31}\text{P}) = 338$ Hz). ^{119}Sn NMR (149.1 MHz, C_6D_6): δ -182.8 (dd, $^1J(^{119}\text{Sn}-^{103}\text{Rh}) = 1172$ Hz, $^2J(^{119}\text{Sn}-^{31}\text{P}) = 338$ Hz). Anal. Calcd for $\text{C}_{53}\text{H}_{65}\text{N}_3\text{PRhSi}_4\text{Sn}$ (1109.0): C, 57.40; H, 5.91; N, 3.79. Found: C, 56.97; H, 5.71; N, 3.56.

[MeSi[SiMe₂N(3,5-xyl)]₃SnIr(PPh₃)(COD)] (8a). A mixture of 400 mg (0.52 mmol) of MeSi[SiMe₂N(3,5-xyl)]₃SnLi(OEt₂) (**2a**) and 158 mg (0.24 mmol) of [IrCl(COD)]₂ was suspended in precooled Et₂O at -78 °C. The orange suspension was stirred for 15 min before it was transferred to 126 mg (0.48 mmol) of PPh₃. While it was slowly warmed to room temperature the color changed to red-brown. Then the solvent was distilled in vacuo and the residue

was extracted with hexane. After removing the solvent in vacuo, a red-brown powder was isolated in 80% (471 mg) yield. FT-IR (KBr-disk): 3020 (w), 2942 (m), 2891 (w), 1598 (s), 1582 (s), 1477 (w), 1434 (m), 1297 (m), 1243 (m), 1158 (m), 1092 (w), 1035 (m), 960 (w), 849 (s), 827 (s), 695 (m), 647 (w), 532 (w) cm^{-1} . ^1H NMR (399.9 MHz, C_6D_6): δ 7.06–6.97 (m, 15H, PPh_3), 6.94 (s, 6H, 2,6- H_{xyI}), 6.59 (s, 2H, 4- H_{xyI}), 5.65 (s, br, 2H, CH_{COD}), 2.68 (s, br, 2H, CH_{COD}), 2.25 (s, 18H, $\text{C}_6\text{H}_3(\text{CH}_3)_2$), 1.85–1.68 (m, 2H, CH_2 COD), 1.60–1.45 (m, 2H, CH_2 COD), 1.33–1.17 (m, 2H, CH_2 COD), 0.78–0.67 (m, 2H, CH_2 COD), 0.59 (s, 18H, $\text{Si}(\text{CH}_3)_2$), 0.27 (s, 3H, $\text{Si}(\text{CH}_3)_2$). ^{13}C NMR (100.6 MHz, C_6D_6): δ 154.8 (s, 1- C_{xyI}), 137.4 (s, 3,5- C_{xyI}), 134.5 (d, $J(^{13}\text{C}-^{31}\text{P}) = 11$ Hz, PPh_3), 133.8 (d, $J(^{13}\text{C}-^{31}\text{P}) = 24$ Hz, PPh_3), 129.7 (d, $J(^{13}\text{C}-^{31}\text{P}) = 2.3$ Hz, PPh_3), 127.9 (d, $J(^{13}\text{C}-^{31}\text{P}) = 10$ Hz, PPh_3 , von C_6D_6), 126.0 (s, 2,6- C_{xyI}), 122.6 (s, 4- C_{xyI}), 75.3 (d, $^2J(^{31}\text{P}-^{13}\text{C}) = 5.2$ Hz, CH_{COD}), 73.3 (d, $^2J(^{31}\text{P}-^{13}\text{C}) = 3.2$ Hz, CH_{COD}), 32.8 (s, CH_2 COD), 21.8 (s, $\text{C}_6\text{H}_3(\text{CH}_3)_2$), 5.0 (s, $\text{Si}(\text{CH}_3)_2$), -14.6 (s, $\text{Si}(\text{CH}_3)_2$). ^{29}Si NMR (79.4 MHz, C_6D_6): δ -1.9 (s, SiMe_2), -96.9 (s, SiMe_2). ^{31}P NMR (161.9 MHz, C_6D_6): δ = 18.1 (s, $^2J(^{31}\text{P}-^{117}\text{Sn}) = 213$ Hz, $^2J(^{31}\text{P}-^{119}\text{Sn}) = 223$ Hz). ^{119}Sn NMR (149.1 MHz, C_6D_6): δ -101.1 (d, $^2J(^{31}\text{P}-^{119}\text{Sn}) = 224$ Hz). Anal. Calcd for $\text{C}_{57}\text{H}_{75}\text{IrN}_3\text{PSi}_4\text{Sn}$ (1256.5): C, 54.49; H, 6.02; N, 3.34. Found: C, 54.81; H, 6.30; N, 3.49.

[MeSi[SiMe₂N(p-tol)]₂[SiMe₂N(2-C₆H₃-4-CH₃)]SnIr(H)(PPh₃)(COD)] (8b). A mixture of 200 mg (0.27 mmol) of MeSi[SiMe₂N(p-tol)]₂SnLi(OEt₂) (**2b**) and 92 mg (0.14 mmol) of [IrCl(COD)]₂ was suspended with precooled Et₂O at -78 °C. The dark red reaction mixture was stirred for 10 min, then a solution of 72 mg (0.27 mmol) of PPh₃ in Et₂O was subsequently added and the reaction mixture warmed to room temperature. After concentration in vacuo and centrifugation, the centrifugate was stored at 10 °C gave dark yellow crystals (528 mg, 80%). FT-IR (KBr-disk): 3060 (vw), 2939 (w), 2891 (w), 2058 (vw), 1604 (w), 1500 (s), 1433 (w), 1235 (s), 1086 (w), 1043 (w), 919 (s), 854 (m), 804 (m), 745 (w), 696 (m), 524 (m) cm^{-1} . ^1H NMR (399.9 MHz, C_6D_6): δ 7.60–7.42 (s, br, 2H, PPh_3), 7.41–7.32 (m, 7H, tol, PPh_3), 7.08–7.01 (m, 7H, tol, PPh_3), 6.98–6.85 (m, 7H, tol, PPh_3), 6.64 (d, 2H, tol), 6.50–6.30 (s, br, 1H, PPh_3), 4.41–4.32 (m, 1H, CH_{COD}), 4.18–4.04 (m, 1H, CH_{COD}), 3.64–3.51 (m, 1H, CH_{COD}), 3.01–2.90 (m, 1H, CH_{COD}), 2.22–2.13 (m, 1H, CH_2 COD), 2.11 (s, 3H, $\text{C}_6\text{H}_4\text{CH}_3$), 2.03 (s, 3H, $\text{C}_6\text{H}_4\text{CH}_3$), 1.94–1.82 (m, 1H, CH_2 COD), 1.78 (s, 3H, $\text{C}_6\text{H}_3\text{CH}_3$), 1.60–1.36 (m, 4H, CH_2 COD), 1.34–1.16 (m, 2H, CH_2 COD), 1.06 (s, 3H, $\text{Si}(\text{CH}_3)_2$), 1.01 (s, 3H, $\text{Si}(\text{CH}_3)_2$), 0.92 (s, 3H, $\text{Si}(\text{CH}_3)_2$), 0.79 (s, 3H, $\text{Si}(\text{CH}_3)_2$), 0.54 (s, 3H, $\text{Si}(\text{CH}_3)_2$), 0.49 (s, 3H, $\text{Si}(\text{CH}_3)_2$), 0.39 (s, 3H, $\text{Si}(\text{CH}_3)_2$), -12.23 (d, $^2J(^{31}\text{P}-^1\text{H}) = 24$ Hz, $^2J(^{117/119}\text{Sn}-^1\text{H}) = 131$ Hz, 1H, SnIr(H)P). ^{13}C NMR (100.6 MHz, C_6D_6): δ 155.3 (s, br, tol_{Ir}), 151.3 (s, tol), 151.1 (s, tol), 143.5 (d, $J(^{31}\text{P}-^{13}\text{C}) = 11$ Hz, PPh_3), 134.3 (d, $J(^{31}\text{P}-^{13}\text{C}) = 9.2$ Hz, PPh_3), 130.5 (d, $J(^{31}\text{P}-^{13}\text{C}) = 33$ Hz, PPh_3), 130.1 (d, $^2J(^{31}\text{P}-^{13}\text{C}) = 9.2$ Hz, P-Ir- $\text{C}_6\text{H}_3\text{Me}$), 130.1 (s, br, tol_{Ir}), 129.7 (d, $J(^{31}\text{P}-^{13}\text{C}) = 2.1$ Hz, PPh_3), 129.6 (s, tol), 128.8 (s, br, tol_{Ir}), 128.3 (s, tol), 128.1 (s, tol), 128.0 (s, tol), 127.8 (s, br, tol_{Ir}), 124.2 (s, tol), 124.1 (s, tol), 124.0 (s, br,

tol_{Ir}), 81.0 (d, $^1J(^{103}\text{Rh}-^{13}\text{C}) = 2$ Hz, CH_{COD}), 80.8 (d, $^1J(^{103}\text{Rh}-^{13}\text{C}) = 4.8$ Hz, CH_{COD}), 73.9 (d, $^1J(^{103}\text{Rh}-^{13}\text{C}) = 6.0$ Hz, CH_{COD}), 71.7 (d, $^1J(^{103}\text{Rh}-^{13}\text{C}) = 2.4$ Hz, CH_{COD}), 36.2, 33.9, 30.1, 29.3 (s, CH_2 COD), 21.0, 20.8, 20.2 (s, $\text{C}_6\text{H}_4\text{CH}_3$), 7.1, 6.8, 2.8, 2.8, 2.4, 1.6, 1.4 (s, $\text{Si}(\text{CH}_3)_2$), -14.6 (s, $\text{Si}(\text{CH}_3)_2$). ^{29}Si NMR (79.4 MHz, C_6D_6): δ 0.4 (d, $J = 1.6$ Hz, SiMe_2), 0.2 (d, $J = 1.8$ Hz, SiMe_2), -2.8 (d, $J = 1.1$ Hz, SiMe_2), -93.2 (s, SiMe_2). ^{31}P NMR (161.9 MHz, C_6D_6): δ 5.5 (s, $^2J(^{117}\text{Sn}-^{31}\text{P}) = 1639$ Hz, $^2J(^{119}\text{Sn}-^{31}\text{P}) = 1713$ Hz). ^{119}Sn NMR (149.1 MHz, C_6D_6): δ -162.5 (d, $^2J(^{119}\text{Sn}-^{31}\text{P}) = 1714$ Hz). Anal. Calcd for $\text{C}_{54}\text{H}_{69}\text{IrN}_3\text{PSi}_4\text{Sn}$ (1214.4): C, 53.41; H, 5.73; N, 3.46. Found: C, 53.67; H, 5.90; N, 3.40.

Crystal Structure Determinations. Crystal data and details of the structure determinations are listed in Table 1. Intensity data were collected at low temperature with Bruker AXS Smart 1000 CCD and Enraf-Nonius Kappa CCD (complex **6b**) diffractometers (Mo K α radiation, graphite monochromator, $\lambda = 0.71073$ Å). Data were corrected for Lorentz, polarization and absorption effects (semiempirical, SADABS).⁴² The structures were solved by the heavy atom method combined with structure expansion by direct methods applied to difference structure factors (DIRDIF)⁴³ or by direct methods (SHELXS-97)⁴⁴ (complex **8b**) and refined by full-matrix least-squares methods based on F^2 with all measured unique reflections.⁴⁴ Due to heavy disorder and fractional occupancy, electron density attributed to solvent of crystallization was removed from the structures (and the corresponding F_{obs}) of **2a**, **3a**, and **5b** with the SQUEEZE procedure,⁴⁵ as implemented in PLATON.⁴⁶ All non-hydrogen atoms were given anisotropic displacement parameters. Hydrogen atoms were generally input at calculated positions and refined with a riding model. When justified by the quality of the data, the positions of some hydrogen atoms (those on the carbon atoms involved in coordination to Rh or Ir, and the hydride in **8b**) were taken from difference Fourier syntheses and refined.

Acknowledgment. This research was supported by the University of Heidelberg and the Fonds der Chemischen Industrie (Germany). We thank the reviewers for helpful comments.

Supporting Information Available: CIF files giving the crystal data for compounds **2a**, **3a**, **4b**, **5a**, **5b**, **6b**, and **8b**. This material is available free of charge via the Internet at <http://pubs.acs.org>.

OM700960P

(42) Sheldrick, G. M. *SADABS*; Bruker AXS, 2004–2007.

(43) (a) Parthasarathi, V.; Beurskens, P. T.; Bruins Slot, H. J. *Acta Crystallogr.* 1983, *A39*, 860. (b) Beurskens, P. T.; Beurskens, G.; de Gelder, R.; Garcia-Granda, S.; Gould, R. O.; Israel, R.; Smits, J. M. M. *DIRDIF-99*; University of Nijmegen: The Netherlands, 1999.

(44) Sheldrick, G. M. *SHELXS-97*; University of Göttingen, 1997.

(45) v. d. Sluis, P.; Spek, A. L. *Acta Crystallogr.* 1990, *A46*, 194.

(46) Spek, A. L. *J. Appl. Crystallogr.* 2003, *36*, 7.